Sādhanā (2021)46:214
https://doi.org/10.1007/s12046-021-01711-3

© Indian Academy of Sciences

Integrating synchrophasor technology for the improvements in system integrity protection schemes under stressed conditions

MAKARAND SUDHAKAR BALLAL[1,*] and AMIT RAMCHANDRA KULKARNI[2]

[1]Electrical Engineering Department, Visvesvaraya National Institute of Technology, Nagpur, India
[2]Maharashtra State Electricity Transmission Company Ltd, Mumbai, India
e-mail: drmsballal@rediffmail.com

MS received 7 October 2020; revised 15 July 2021; accepted 17 July 2021

Abstract. The power transmission system, in this age, is characterized by ultra- and extra-high voltage AC, and multi-terminal high voltage DC networks. It has a wide-area power network across the nation. It incorporates conventional and ultra-mega-power plants (UMPPs). It also has a submission of increasing penetration due to Renewable Energy Sources (RES). A crucial role is delivered by the system integrity and protection schemes (SIPS) in sustaining guaranteed and safe grid operation. A SIPS also assists efficient grid management during serious power system emergencies. In this article, thorough investigation of the performable capabilities of three influential SIPS in India is made. The shortcomings in ongoing SIPSs got revealed. A proposed methodology eliminates these obstacles. Apperception and vitality of the recommended technique get decided by simulation exercise on an IEEE 10 generators 39-bus test system ingrained with HVDC link in MATLAB. Simulation outcomes accomplished the credibility of the method in defending system integrity. Electrical Transient Analyzer Program (ETAP) is used for the validation of MATLAB results. ETAP has an organizing/investigation mechanism and it is a remarkably convenient interface.

Keywords. Functional investigation; system integrity and protection schemes (SIPS); power swing; distance relay; test system; MATLAB; ETAP.

1. Introduction

System integrity protection schemes (SIPS) are strategies that can act under consternation and avert a total failure of an electrical power network. The main objective of SIPS is to monitor the state of the electricity transmission network in actual time and revert it in exigency conditions. Attainment of efficient execution of SIPS resolves the threat before the research community. In literature, diverse approaches and procedures have explained the advancement in SIPS [1–5]. A joint compendium of IEEE and CIGRE to regulate the SIPS regarding the authenticity of performance is in [6]. It covers the design and the reliability norms used for the development of expected SIPS. Online demonstration of a new response-based (feedback) Wide-Area stability and voltage Control System (WACS) is discussed in [7]. The control system comprises phasor measurements at many substations using diversified behavior for power system equilibrium. In [8], an adaptive fault location technique based on phasor measurement units (PMUs) for the electricity transmission line provides data of voltage and current phasors of end terminals of the transmission corridor. The online system's parameters of the electricity transmission line determine the faulty section. Article [9] depicts several PMU-based protection and control systems. They include a synchrophasor for alternator shedding and backup protection for earth faults. Two extensive disruptions: (i) forced outages on generation units and (ii) load dislocations, were reported in [10]. A Wavelet method is applied to access the frequency and voltage characteristics for the event analysis.

Article [11] gives computational and analytical augmentation for power transmission networks due to faults. It connects an online as well as an offline stage. The time measurements of traveling waves promulgating from the fault point support the online analysis. A critique of SIPS applied in the power system of Norway along with its preservation assessment study carried on the IEEE reliability-proved system is discussed in [12]. However, these SIPS did not give admirable solutions. A procedure explained in [13] is to design SIPS for a tradeoff between security and prominence. It adopts fault-tree reasoning and the concept of nominal cut sets to disseminate the reliability analysis of the complete SIPS into the individual operational phases of SIPS. The fault location technique given in [14] uses sparsely positioned wide-area phasor measurements. It gave the model of the abnormal system. The equivalent terminal bus injections depicted the same

*For correspondence
Published online: 19 October 2021

changes in bus voltages with the abnormal current measured at any point on the faulted line. Thus it requires an appropriate network model and a proportionate number of phasor measurements for the network. A specific SIPS described in [15] is for enhancing the security of protection activity. Impressionable points, which may cause false trippings under a stressed condition, are identified. The false trippings could be avoided by including a protection scheme. In [16], a few significant threats were resolved for better performance of the protection system. It covers cascade trippings and wide-area disruptions, blackouts, and the security of backup relays in the more complex operating conditions. Currently working SIPS and their state of the art and coordinated protection system vested on inter-substation data are reported in [17]. In [18], root mean square (RMS) values from time-synchronized voltage and frequency of architecture determine coefficients determined by regulated Wavelet energy function. However, it regresses the non-stationary incidence of alterations in signals. A procedure given in [19] is to ingress the risk of SIPS false operations and inadmissible interactions among different SIPS on similar or adjacent systems. These SIPS, with robust protection logics, accommodate the increasingly variable system contexts and the performance of associated protection schemes.

The frequency phasors of current and voltage have some facets described in [20]. They can segregate between power swings and short-circuit faults. In this, the features extracted from alternator models are contemplated in stability studies. A blackout is addressed in [21] at the ultra-mega-power project (UMPP) in a western region (WR) grid of India infuriated by the action of protection relay under power swing. Also, to alleviate instability because of unstable power swing, a SIPS has been invented. SIPS in [22] impelled relay security indices from the apparent impedance. They are used to rule out the zone-3 wrong operations of protection elements under contingencies. This approach does not require coherency group assimilation. It remains impartial for the revision in network topology but functions for only stable swing contingencies. The performing attributes executed in [23] demonstrated the modal current correlation plane. However, this arrangement is restrained to dual power circuits. In [24], dedicated SIPS

Table 1. Indian power grid overview [31].

SN	Particulars	Quantity
1	Generation installed capacity	378 GW
2	Transmission line above 220 kV	381671 ckm
3	Transformation capacity above 220 kV	791570 MVA
4	Renewable energy installed capacity	65 GW
5	HVDC bipolar/B to B systems	11 nos.
6	Multi-terminal DC (MTDC)	1
7	SIPS in operation	52

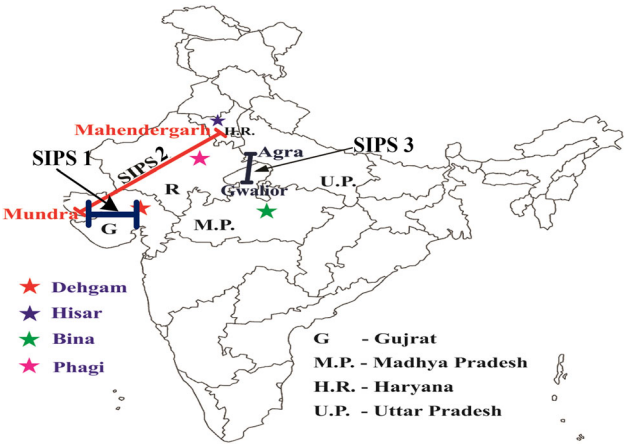

Figure 1. SIPSs under study.

architecture is manifested for augmented achievability and flexibility based on PMU technology. However, the maximum possible power flow due to this SIPS was not examined. A pilot scheme for the secured operation of zone-3 under stressed system conditions is checked in [25]. It delivered on the New England 39-bus system. However, it mandatorily requires the communication bandwidth for correct operation. Article [26] provides an overview of the structure and applications of wide-area monitoring, protection, and control (WAM-PAC) system that serves as SIPS to monitor, control, and protect the transmission network during ordinary and unusual operating conditions. The application of the PMU mechanism reported in [27] depicted the development of SIPS as a part of the WAM-PAC arrangement. Here, the optimal bus breaking scheme identifies necessary actions that can eliminate or reduce power system overloads. Thus, it assures the integrity of the power system.

Model prognosticative control maneuver is discussed in [28]. It repeatedly amends the power stunts (set points) of MTDC converter stations and generating units to alleviate overloads. In this, the controller is for the typical automatic power control. PMUs fault detector technique is ratified for a transmission line. However, the extant SIPS need PMUs. A PMU-aided SIPS for power transmission network is described in [29]. It exploits synchronized voltage phasor and current phasor information from all PMUs. It has operated to detect the disturbance, identify a disturbed area, and locate the sensitive region. Thus, it tries to improve the situation awareness. A cyber-attack buoyant safeguard scheme described in [30] is operated by multi-agents. Here, a state-responsive protocol is applied to expedite data interchange with agents. Thus, the disorganized protection arrangement has more pliancy and affability when facing venomous attacks compared with traditional protection. This article presents the participation of some SIPS executed in India and their realization. The uniqueness of this research paper is as follows:

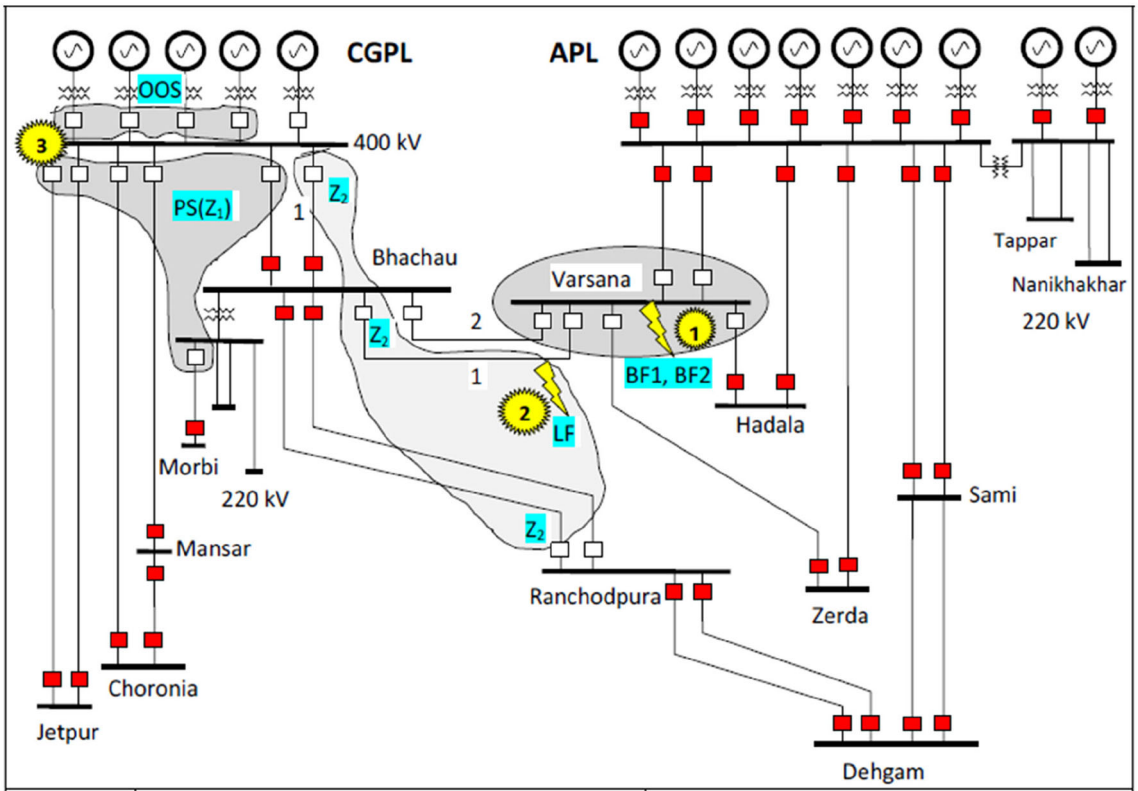

Time	Fault	Event
20:29 hrs	Bus fault (BF1) at 400 kV Bus-1 of Varsana 440 kV Substation	Elements connected to 400 kV Bus-1 & 2 got disconnected.
21:50 hrs	Bus fault (BF2) at 400 kV Bus-2 of Varsana 440 kV Substation	
02:37 hrs	Bhachau-Versona-1 line charged from Bhachau end	Line fault (LF) sensed by Distance Relay in Zone-2 at Bhachua end of the line and further at 1. Ranchdopura end of Bhachau-Ranchodpura lines 2. CGPL end of CGPL-Bhachau-1 line; the lines tripped.
02:37 hrs	Subsequently, power swing (PS) in Zone-1 sensed by Distance relays of remaining five lines at CGPL end.	All five lines tripped. At the same time, Generating units at CGPL tripped on Out of Step (OOS)

Figure 2. One-line diagram with a sequence of occurrence at CGPL [21].

Table 2. Details of SIPS-1 operation [32].

SN	Triggering event	Action plan
1	If exports exceed 3100 MW and any one of the lines trips or if loading is above 900 MW	Decrease generation of two units to 800 MW
2	If exports exceed 3100 MW and if CGPL–Bhachau twin-circuit line trips	Remove one unit immediately from system
3	If CGPL–Bhachau double-circuit line trips, CGPL–Jetpur or combination of any one circuit of Bhachau or Choronia or Jetpur trips	Back down generation to 800 MW such that the loadings of rest of the lines are below 900 MW

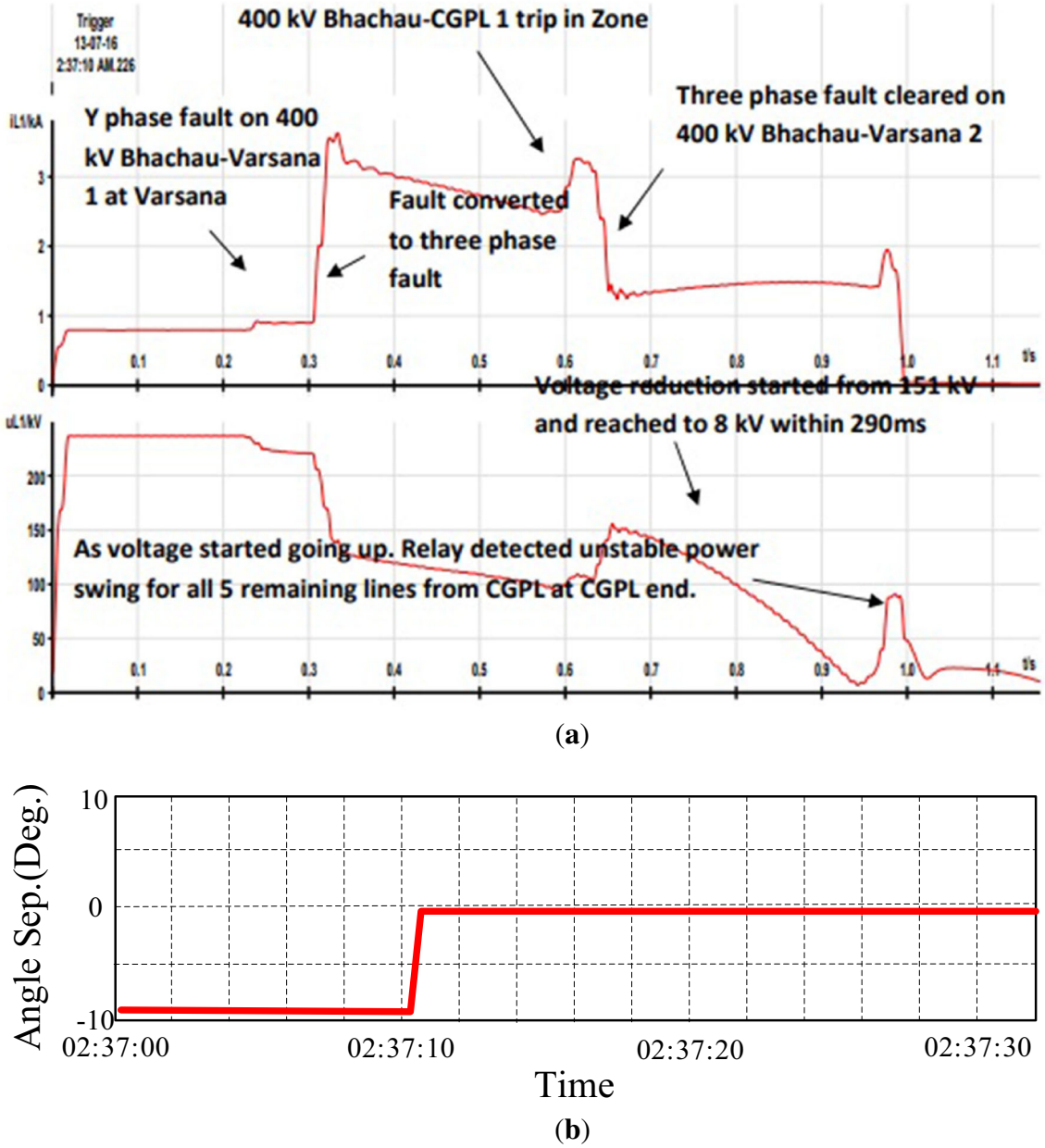

Figure 3. PMU data retrieved at 400 kV CGPL–Bhachau Line 2: (**a**) voltage and current, and (**b**) angular separation at CGPL [32].

(i) Three existing SIPS in the northern (NR) and western regions (WR) of India have been assessed.
(ii) IEEE 10-generator 39-bus system is accomplished and ingrained with HVDC line in technical computing software MATLAB and performance of all three SIPS tested.
(iii) The disparities of prevailing SIPS are enumerated.
(iv) The methodology is suggested to overcome these disparities by two subroutines.
(v) Working current SIPS in coordination with recommended methodology were inspected.
(vi) MATLAB simulation results are justified by comparing them to the Electrical Transient Analyzer Program (ETAP) results.
(vii) The evaluation of online performance was carried out based on information from a wide area. It incorporates the intelligent control responses through an intended algorithm

The advantages of the proposed methodology are that it is applied to any SIPS and requires PMU data for execution. It does not demand any previous or historical data and assessment procedures. Measurements by PMU facilitate the SIPS to refrain from arduous electrical network

Table 3. Details of SIPS-2 operation [32].

SN	Triggering event	Action plan
1	Blocking of one pole and reduction in power submissionat Mahendergarh between 600& 900 MW	Load shedding 320 MW in NR: Haryana (140 MW), Punjab(60 MW), Rajasthan (60 MW), and Uttar Pradesh (60 MW).Trip generating unit 1 at CGPL, Mundra Power Plant
2	Blocking of one or both pole and decrement in powersubmission at Mahendergarh between 900& 1250 MW	Load Shedding 650 MW in NR: Haryana (320 MW) along with Punjab, Rajasthan, and Uttar Pradesh (110 MW each). Trip generating unit 1 and back down generating unit 2 at CGPL,Mundra Power Plant
3	Blocking of both poles and change in power submission at Mahendergarh between 1250 & 2000 MW	Load shedding 1350 MW in NR: Haryana (550 MW) along with Punjab, Rajasthan, Uttar Pradesh, and Delhi (200 MW each). Trip generating unit 1 and 2 and back down generating unit 3 at CGPL, Mundra Power Plant
4	Blocking of both poles and change in power submission at Mahendergarh by more than 2000 MW.	Load shedding 1850 MW in NR: Haryana (650 MW) along with Punjab, Rajasthan, Uttar Pradesh, and Delhi 300 MW each. Trip generating unit 1, 2, and 3 and back down generating unit 4 at CGPL, Mundra Power Plant

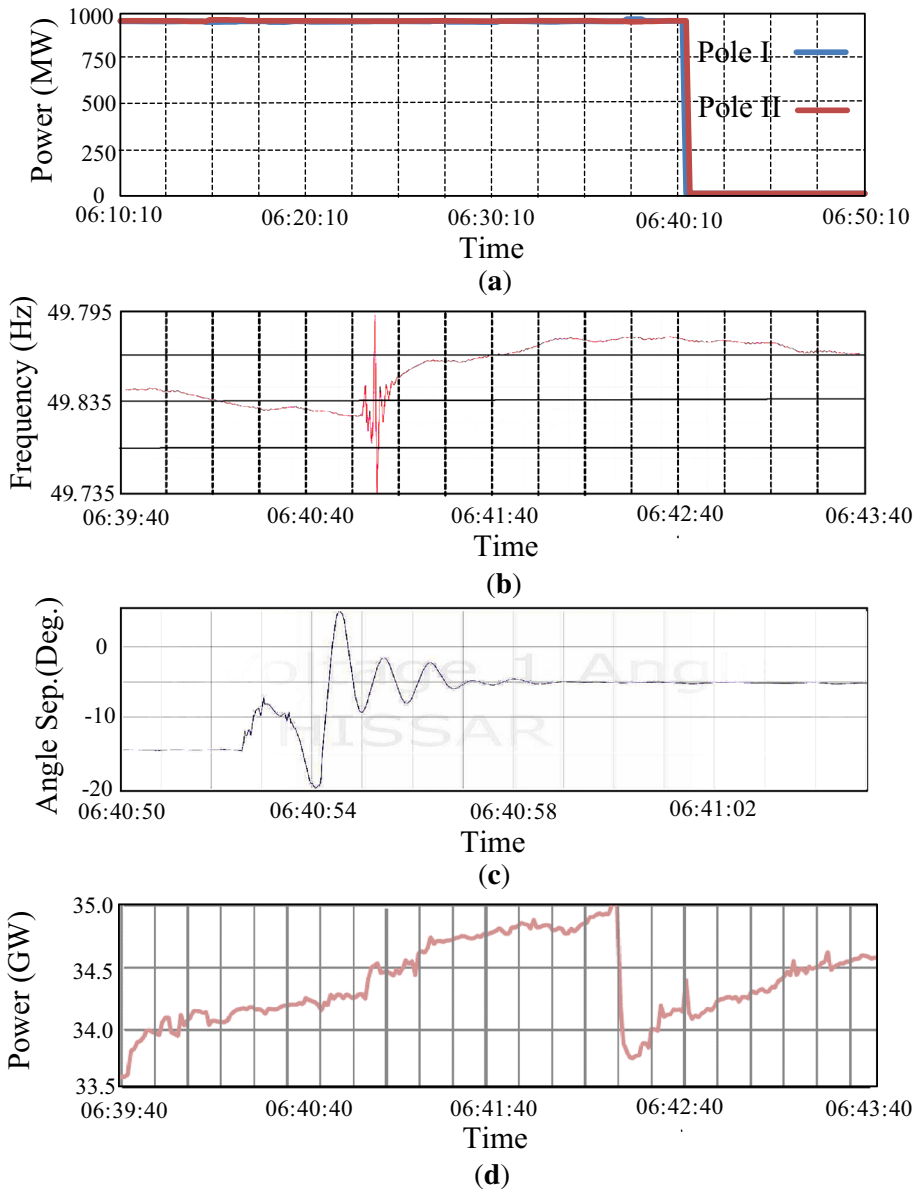

Figure 4. PMU data retrieved for SIPS-2: (**a**) power flow variation due to HVDC pole tripping, (**b**) frequency variation at CGPL–Mundra PMU, (**c**) angular separation, and (**d**) load shedding in NR [32].

Table 4. Details of SIPS-3 operation [32].

SN	Triggering event	Action plan
1	If import by NR is within 1000–1500 MW on 765 kV Agra–Gwalior Circuit 1 and 2	Back down generation of two units to 520 MW
2	If import by NR is greater than 1500 MW on 765 kV Agra–Gwalior Circuit 1 and 2	Load shedding 1150 MW in NR

modeling. Thus this reduces potential errors, and the accuracy of operation achieved is more than 95%. This coordination with extant SIPS gives close-loop control and makes the scheme robust. A prospective algorithm can tackle any normal and abnormal conditions. The remainder of this paper is as follows. Section 2 describes the functional assessments of three currently working SIPS in India. The methodology recommended to beat the drawbacks in

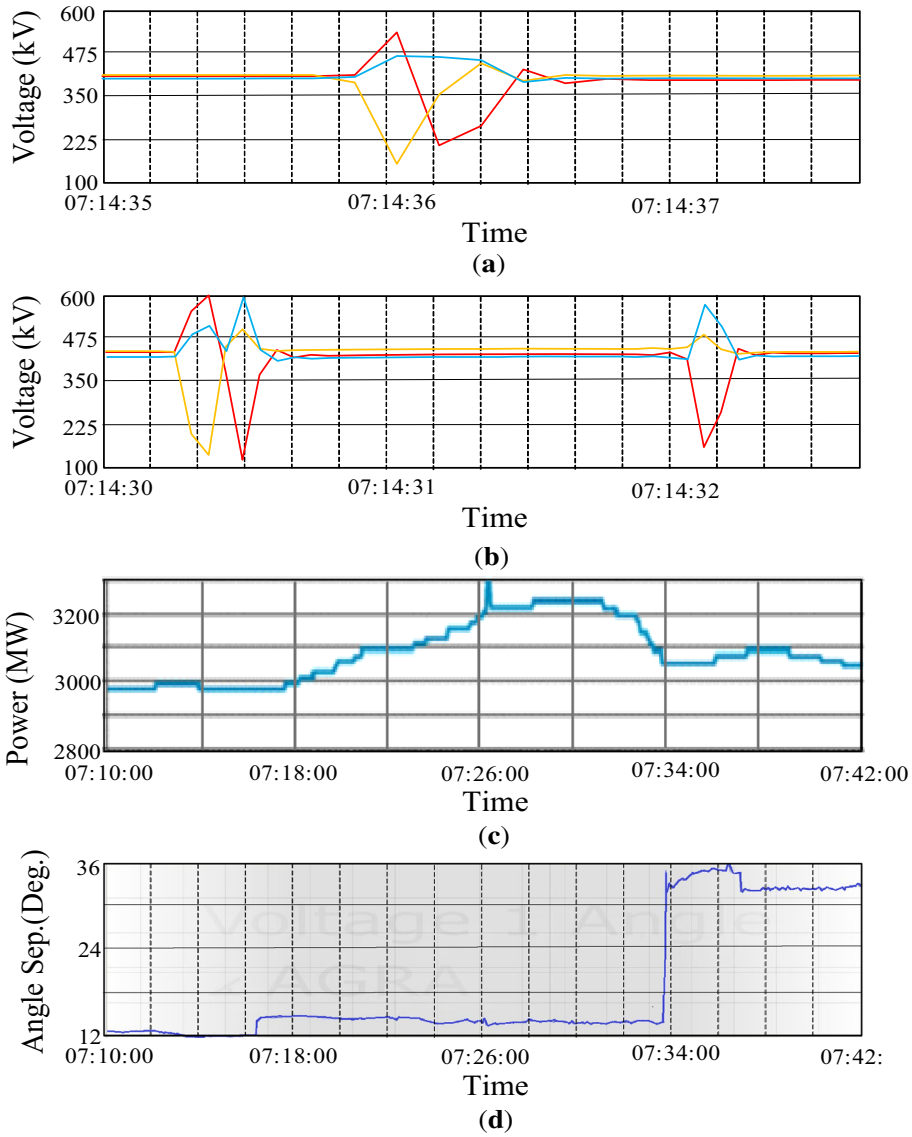

Figure 5. PMU data retrieved for SIPS-3; voltage dip after a trip of 765-kV Gwalior–Agra: (**a**) Circuit 1, (**b**) Circuit 2, (**c**) generation back-down at CGPL–Mundra, and (**d**) angular separation observed by Agra PMU.

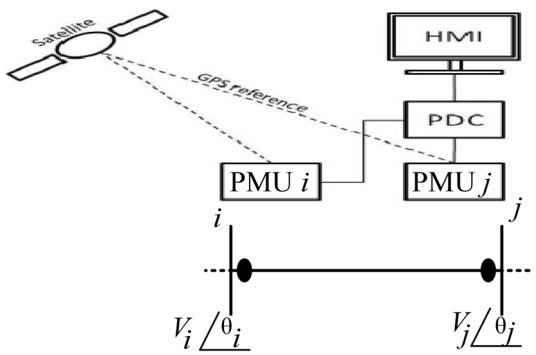

Figure 6. Application of PMU for SIPS improvement.

these SIPS is explained in Section 3. In Section 4, the comparison among the MATLAB simulation results and corresponding ETAP results validates the performance. The conclusion is in Section 5.

2. Functional assessment of current SIPS

India is an extensive electric power producer and consumer in the world. The Indian Power system comprises five provincial grids for operational and planning purposes. In the last century, the Indian national grid fabrication was completed with the territorial power networks. The consolidation of territorial grids beginning with asynchronous HVDC back-to-back union encourages an exchange of power between the provinces. A critique of the Indian power grid as of January 2021 is in table 1. Fifty-two SIPS perform in India. These SIPS are used to

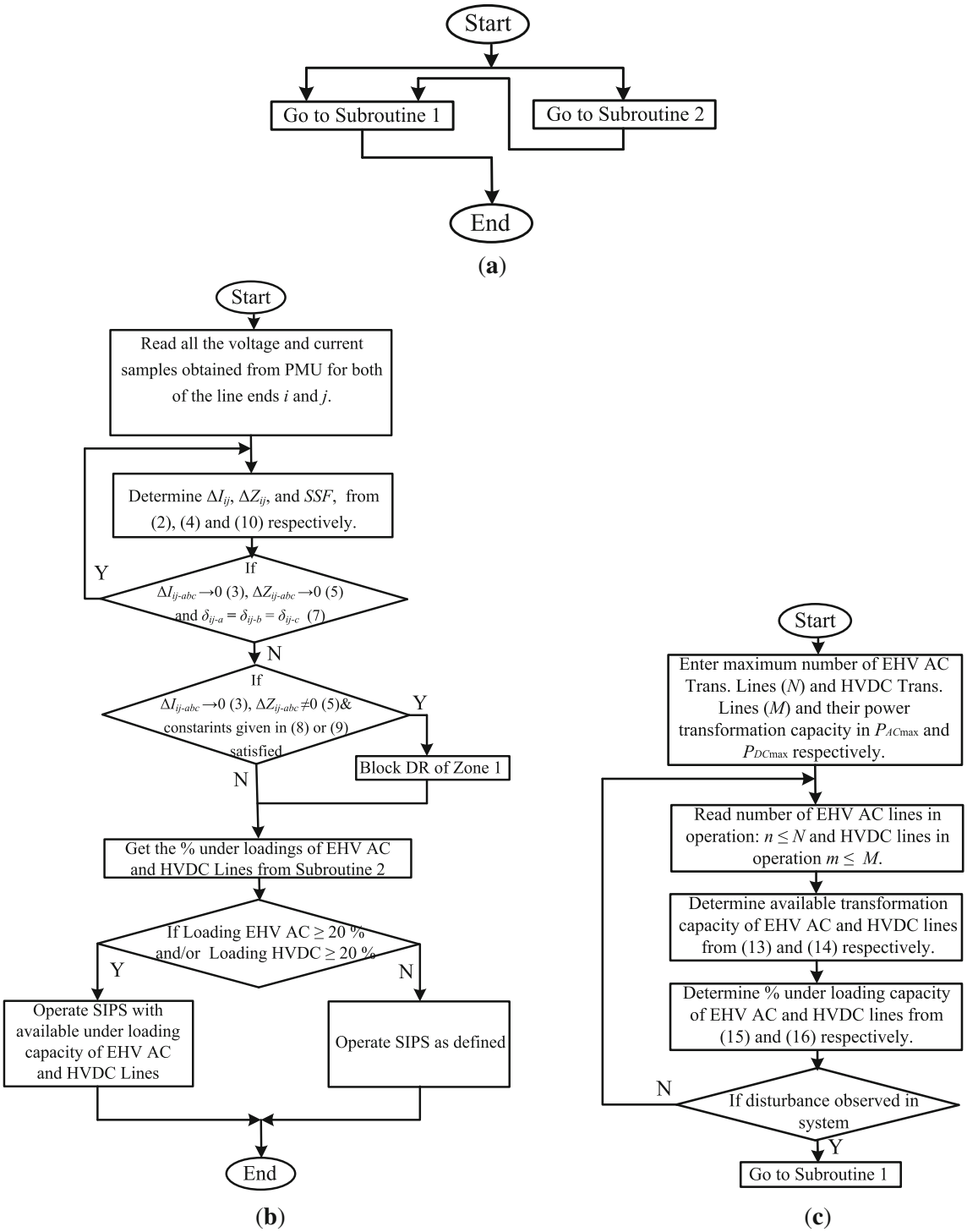

Figure 7. Proposed methodology: (**a**) main flow chart, (**b**) subroutine 1, and (**c**) subroutine 2.

perform certain specific tasks. It considers the opening of critical transmission lines, secure discharge of generation, overriding transformers, backing down of generating units, etc. Three incidences in the Indian power grid motivate the authors to write this article. Figure 1 illustrates SIPSs under conversation. Their performances are analyzed.

2.1 *Blackout at CGPL - UMPP, India, on 13th July 2016*

A private power project in Kutch district near Mundra Port (Gujarat) is India's most energy-proficient thermal plant. This ultra-mega-power plant (UMPP) managed by M/s. Tata Power is known as Coastal Gujarat Power Limited

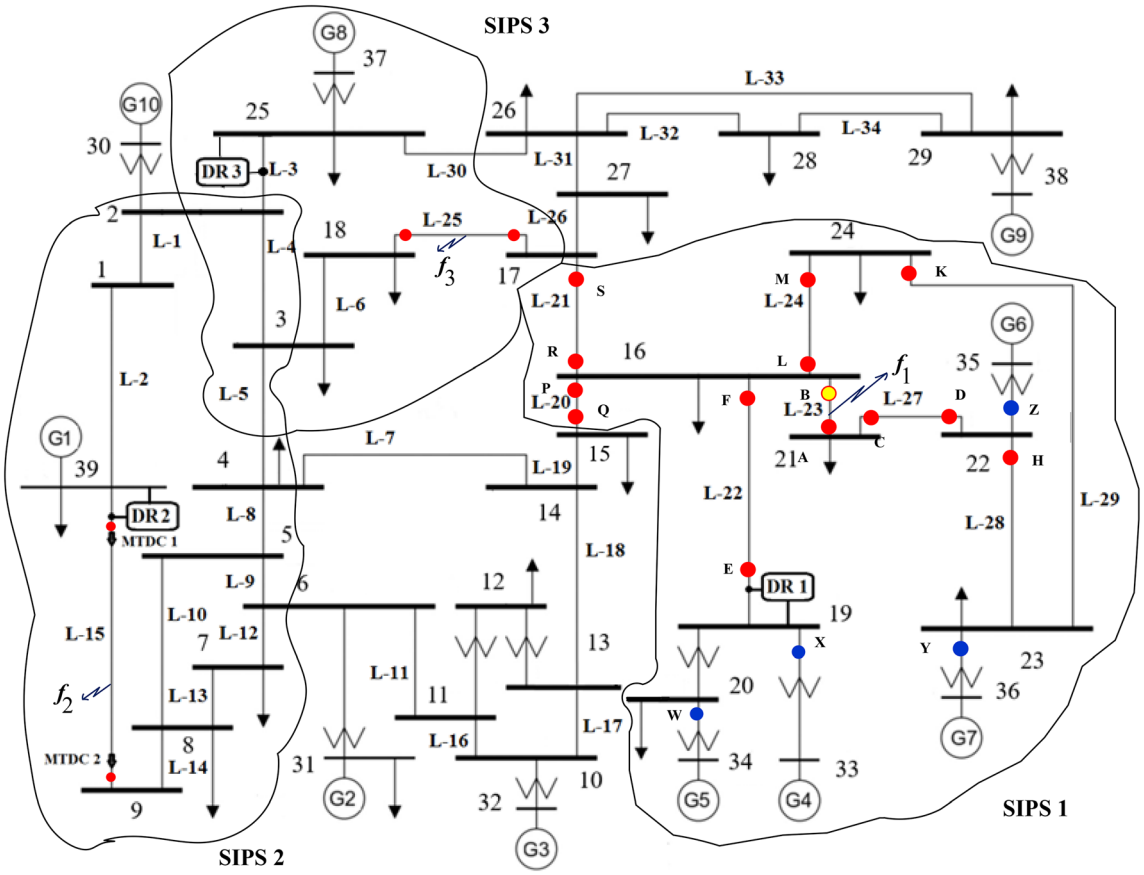

Figure 8. IEEE 10 generators 39-bus test system ingrained with HVDC link.

Table 5. Generation and load connected to IEEE 39-bus New England system embedded with a HVDC link.

	Generation			Load			Load	
Bus no.	*P* (MW)	*Q* (MVAR)	Bus no.	*P* (MW)	*Q* (MVAR)	Bus no.	*P* (MW)	*Q* (MVAR)
30	200	50	3	310	10	23	260	120
31	250	60	4	520	70	24	300	70
32	620	200	7	210	70	25	210	60
33	590	–80	8	410	280	26	150	30
34	550	180	12	10	90	27	270	–80
35	630	210	15	300	80	28	220	40
36	580	120	16	345	45	29	300	30
37	500	180	18	155	30	31	10	5
38	840	40	20	620	120	39	1090	240
39	1000	110	21	285	100			

(CGPL). It administrates five generating units of 800 MW. Power by this project is supplied to three states in WR (Rajasthan, Gujarat, and Maharashtra) and two states in NR (Punjab and Haryana). A blackout happened at CGPL on 13^{th} July 2016 due to an unstable power swing [32]. The one-line diagram (OLD) of this event with disturbances is shown in figure 2 for 400 kV substations. SIPS-1 is intended to act under contingencies. It came into action under abnormal conditions. The course of action for SIPS-1 is in table 2. CGPL was generating 2875 MW before this occurrence. Two consecutive faults on bus 1 and 2 at the Varsana substation infuriated these crises. The previous fault occurred at 20:29 Hrs. and a successive fault occurred on bus 2 at 21:50 Hrs. It led to a blackout of the 400 kV

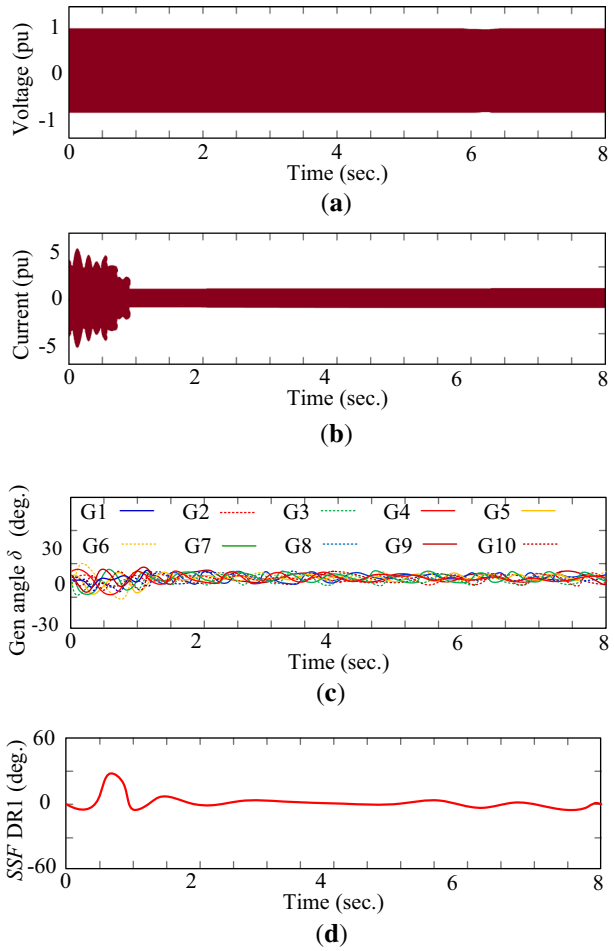

Figure 9. Functional investigation of SIPS-1 under normal condition: (**a**) voltage monitored by DR1, (**b**) current seen by DR1, (**c**) variations in the angles of generating units, and (**d**) *SSF* within bus 16 and 19.

Varsana substation. After closing the circuit breaker of the Bhachau–Varsana-1 transmission line from the Bhachau end, a line fault in zone-2 appeared in the relays at Bhachua, Ranchdopura, and CGPL substations.

At the time of occurrence, CGPL generation delivered power to the Varsana substation. It is there in the disturbance records. After closing circuit breakers of Bhachua–Varsana line 1, at 350 ms, the opening of 400 kV lines with a perpetual decline in bus voltage for 290 ms was noticed. A voltage enhancement appeared at the CGPL end. Thus, power swings impinge in zone-1 of all the lines. Respective distance relays (DRs) sense it. Then they issue a trip command to the corresponding circuit breakers. It resulted in an unstable power swing and the oscillations did not damp. Subsequently, out-of-step (OST) protection got activated for the CGPL alternators. It results in a 2875 MW generation loss. Figure 3(a) gives the voltage and current before and after the fault. It illustrates that the problematic section is disconnected. The fault is attended for 400 kV Bhachau–Varsana line 2. However, due to the disturbance inserted by unstable power swing, the system did not acquire stable condition. The voltage variation was recorded from 151 to 108 kV within 290 ms.

Power swing was identified by DR of five lines emanating from CGPL. Angular disengagement at the time of occurrence is in figure 3(b). The expert study group made transient stability studies reported in [32]. The consultation made by this study group consists of the following: (i) employment of line differential relaying because critical fault clearance time was 100 ms; (ii) zone settings of distance relay under power swing encroach just after the fault are very high; (iii) unstable power swing observed in simulation studies is due to disconnection of one generating unit at CGPL alleviating the oscillations and extending fault clearance by 300 ms; and (iv) modification is necessary for currently operating SIPS. The task force appointed after the 2012 Indian blackout had endorsed block and de-block feature activation in distance relay during power swing.

2.2 *Bipolar HVDC link tripped on 8th January 2016*

The first ±500 kV HVDC bipolar line in India is 960 km long and transmits 2500 MW power as depicted in figure 1. This line traverses power from the WR (Mundra) to the NR (Mahendergarh). The SIPS employed to operate in contingency is given in table 3. It responds in two ways: one for backing down of generation at Mundra and second for predefined load shedding in the NR. On 8th January 2016 at 6:40 Hrs., this HVDC link tripped on earth fault. Mahendergarh was importing 1800 MW as each pole was transmitting 900 MW. Figure 4(a) shows the sudden change in power due to tripping. The fluctuation in system frequency was from 49.73 to 49.98 Hz as seen in figure 4(b). The hike in frequency by 0.1 Hz (49.85 to 49.95 Hz) caused load loss due to this occurrence. The bus voltage fluctuations appeared for 10 s. Due to this sudden load dislocation in NR, the angular estrangement between the WR (Dehgam substation) and NR depressed by 10 degrees. Figure 4(c) illustrates this deviation. Due to the interruption of the HVDC line, there was an enhancement in the power flow on neighboring 765 kV lines. The exclusive SIPS employed under the opening of the HVDC line came into action for proper grid management. The control action trips the two generating units and reduces the generation of a third generating unit at Mundra. It also imposed 1400 MW load shedding in the NR, see figure 4(d). Associated SIPS gave correct performance under this stressed condition.

2.3 *Twin circuits between WR and NR forced under outage on 14th January 2016*

The 765-kV superpower highway is Sipat (WR)–Seoni (WR)–Bina (WR)–Gwalior (WR)–Agra (NR)–Fatehpur

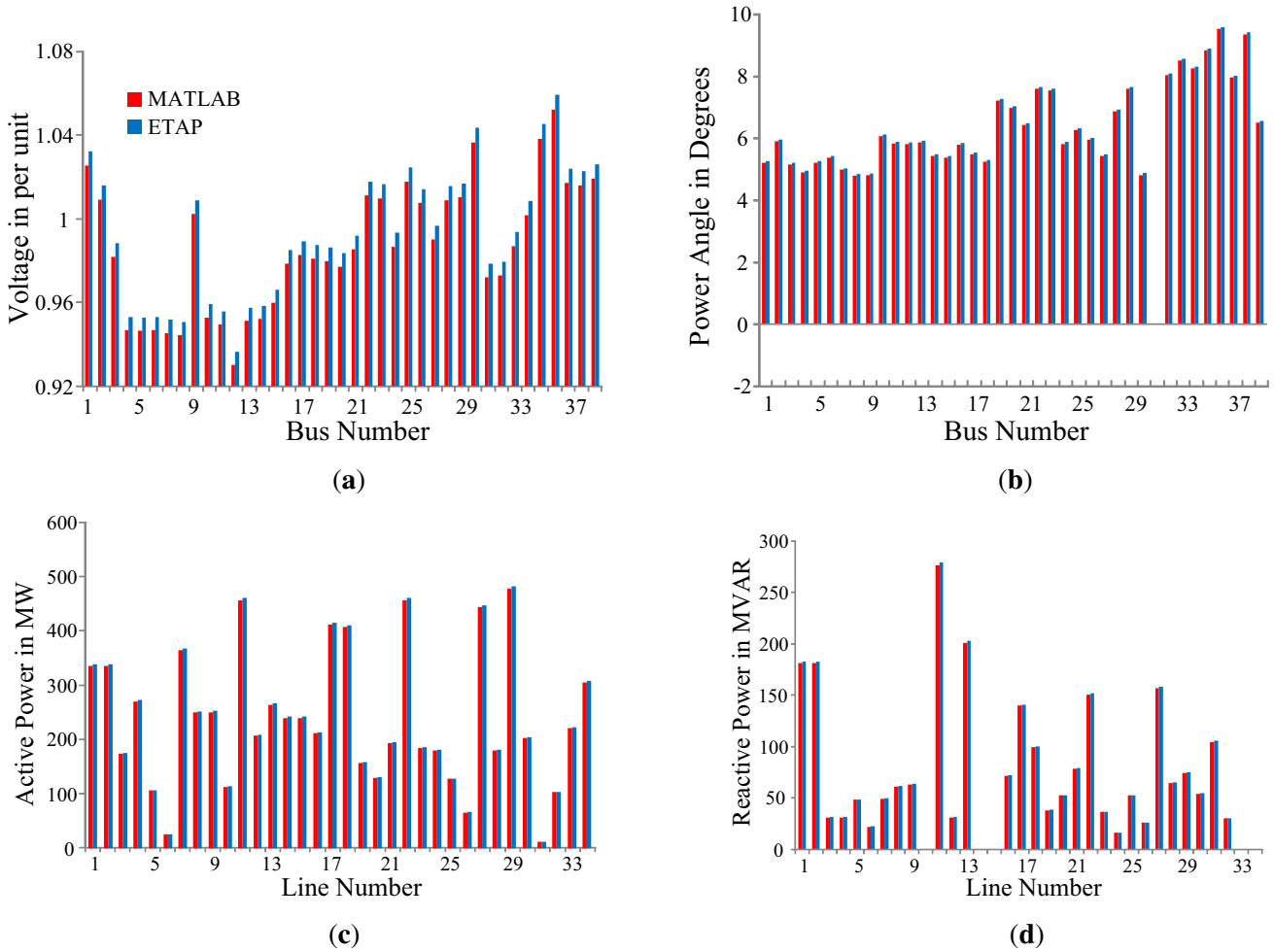

Figure 10. MATLAB and ETAP results for the normal condition: (**a**) bus voltage, (**b**) power angle, (**c**) active power flow, and (**d**) reactive power flow.

(NR)–Sasaram (NR)–North Karanpura (ER)–Sipat (WR) 765 kV Agra–Gwalior–Bina governed at 400 kV. This transmission corridor is in operation since March 31st, 2007. It provides an inter-regional synchronous link within the NR and WR grid. PMUs installed at 400 kV sub-stations, 765 kV sub-stations, and major power plants with fiber-optic (FO) communication promote regulation, control, and situational awareness of the power grid. Customized SIPS-3 is activated at Gwalior (WR) for corrective measures of such events. It is used under contingency and prevents grid disturbances. Table 4 gives its course of action.

On 14th January 2016, in the early morning, dense fog was in northern parts of India. Some 400 kV lines were under maintenance outages. Mundra–Mahendergarh HVDC link was operating with a restricted power flow of about 1000 MW. As recorded by Agra PMU, the L-G fault on phase-*b* tripped 765 kV Gwalior–Agra Circuit 2 at 07:14 Hrs. Bus voltage momentarily dropped to 155 from 430 kV. This tripping boosted the power flow of 765 kV Gwalior–Agra Circuit 1 to 2300 MW. At 07:30 Hrs., 765 kV Gwalior–Agra Circuit 1 tripped on phase-*b* to ground fault. Agra PMU recorded the optimum voltage dip in phase-*b*. This tripping increased the angular separation to 34 degrees from 17 degrees between Bina (WR) and Agra (NR) terminals. After this tripping, dedicated SIPS came into action and forced load shedding of 1200 MW in NR (Punjab, Haryana, UP, and Rajasthan). It backed down the generation of 180 MW at Mundra, 145 MW at Korba Thermal Power Station (KTPS), and 250 MW at Vindhyachal. This SIPS-3 strategy is seen in figure 5. The functional investigation made in this section is about the three existing SIPS. SIPS-1 did not give an intended performance under contingency. Therefore, the CGPL turned dark. However, SIPS-2 and SIPS-3 operated correctly. They gave a satisfactory performance. However, they got influenced due to excessive load shedding, forced outages of generating units, and backed down generation. The following section suggests a methodology to resolve these discrepancies.

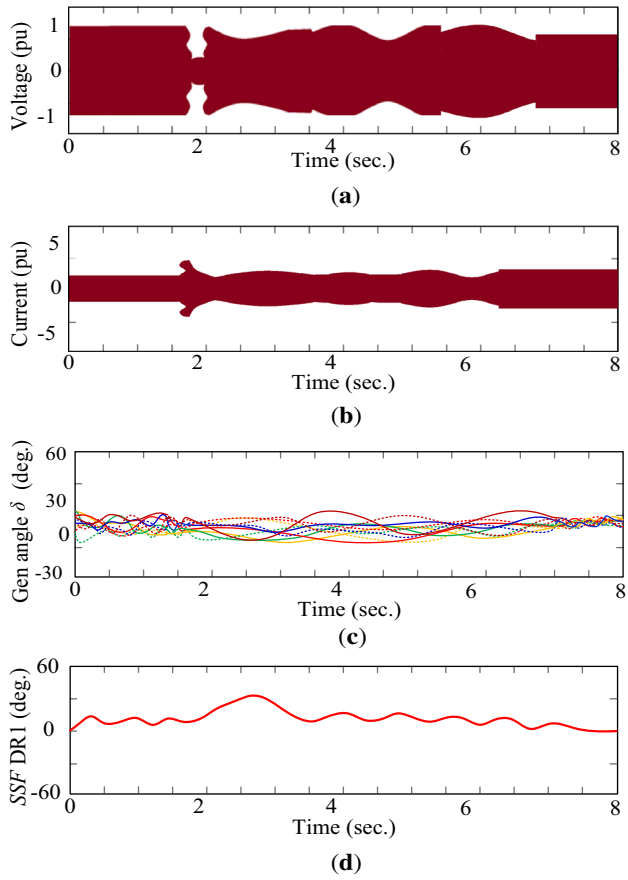

Figure 11. Functional investigation of SIPS-1 under stable swing condition: (**a**) voltage monitored by DR1, (**b**) current seen by DR1, (**c**) variations in the angles of generating units, and (**d**) *SSF* within bus 16 and 19.

3. Improvement in the performance of currently working SIPS

The repulsive opening of power transmission lines because of power swings, exaggerated load curtailment, and derated operation of alternators are the issues conferred in the previous sections. In this section, a methodology is apprised to settle these issues using PMU technology. PMU is a synchrophasor device used to determine the magnitude and phase of an electrical quantity, *viz*. voltage or current at specific locations. Figure 6 delineates a part of the power grid. By connecting PMUs at ends (i and j), it is possible to collect practical voltage samples $v(t)$ and current samples $i(t)$. An algorithm of three sample techniques was applied to determine voltages V_i and V_j, currents I_i and I_j, and their corresponding phase angle θ_i and θ_j. The small changes in voltage and current are

$$\Delta V_{ij-abc} = V_{i-abc} - V_{j-abc} \tag{1}$$

$$\Delta I_{ij-abc} = I_{i-abc} - I_{j-abc} \tag{2}$$

It has to be noted that ΔI_{ij-a} , ΔI_{ij-b}, and ΔI_{ij-c} are zero during power swing.

$$\Delta I_{ij-a} = \Delta I_{ij-b} = \Delta I_{ij-c} = 0 \tag{3}$$

However, in L-G fault (phase-a to ground) in power swing, $\Delta I_{ij-b} = \Delta I_{ij-c} = 0$ and $\Delta I_{ij-a} \neq 0$. This irregularity identifies the faulty phase. The variation in impedance found by the distance relay at the end i is

$$\Delta Z_{ij-abc} = \frac{\Delta V_{ij-abc}}{I_{i-abc}} \tag{4}$$

The rate of change of ΔZ_{ij-abc} is constant in the power swing. Thus, the differential impedance is zero. It is given as

$$\Delta Z_{ij-a} = \Delta Z_{ij-b} = \Delta Z_{ij-c} = 0 \tag{5}$$

However, PMU data giving angle deviations under forced outages is the important parameter for perfect monitoring. This angular displacement of voltage phasors acts as an initial indicator of system stability. The small angular deviation between bus i and bus j is given by

$$\delta_{ij-abc} = \theta_{i-abc} - \theta_{j-abc} \tag{6}$$

$$\delta_{ij-a} = \delta_{ij-b} = \delta_{ij-c} \tag{7}$$

Condition (7) is satisfied only if power swing is exhibited. However, during power swing, if L-G fault exists, $\delta_{ij-a} < \delta_{ij-b} = \delta_{ij-c}$. This constraint selects the faulty phase. The correlation with the rate of δ_{ij-abc} for predefined time interval T detects power swing. It signifies a stable power swing if it is less than T

$$\delta_{ij} \geq \delta_{ij(min)}, \ldots\ldots\ldots t \leq T \tag{8}$$

where $\delta_{ij} = (\delta_{ij-a} + \delta_{ij-b} + \delta_{ij-c}) \div 3$. If this rate of change of δ_{ij} is higher than T, it signifies an unstable power swing

$$\delta_{ij} \geq \delta_{ij(min)}, \ldots\ldots\ldots t \geq T. \tag{9}$$

The variation in impedance for all three zones given in (4) is compared to its thresholds. The respective thresholds of zone-1, zone-2, and zone-3 are ΔZ_1, ΔZ_2, and ΔZ_3. It could be possible that the impedance estimated by relay ΔZ_{ij} can be less than its set value during power swing. Therefore, to distinguish the fault and power swing, the incremental ΔI_{ij} is determined from (2). These differential currents approaching zero implies no-fault in line and the change in ΔZ_{ij} is because of power swing. This constraint is added in protection relays to avert false tripping. The system stability factor (*SSF*) gives the disparity between utmost angular separation $\delta_{ij(max)}$ and actual δ_{ij}

$$SSF = \delta_{ij(max)} - \delta_{ij} \tag{10}$$

This *SSF* should be as low as possible for better system stability. The prime objective of this exploration is to

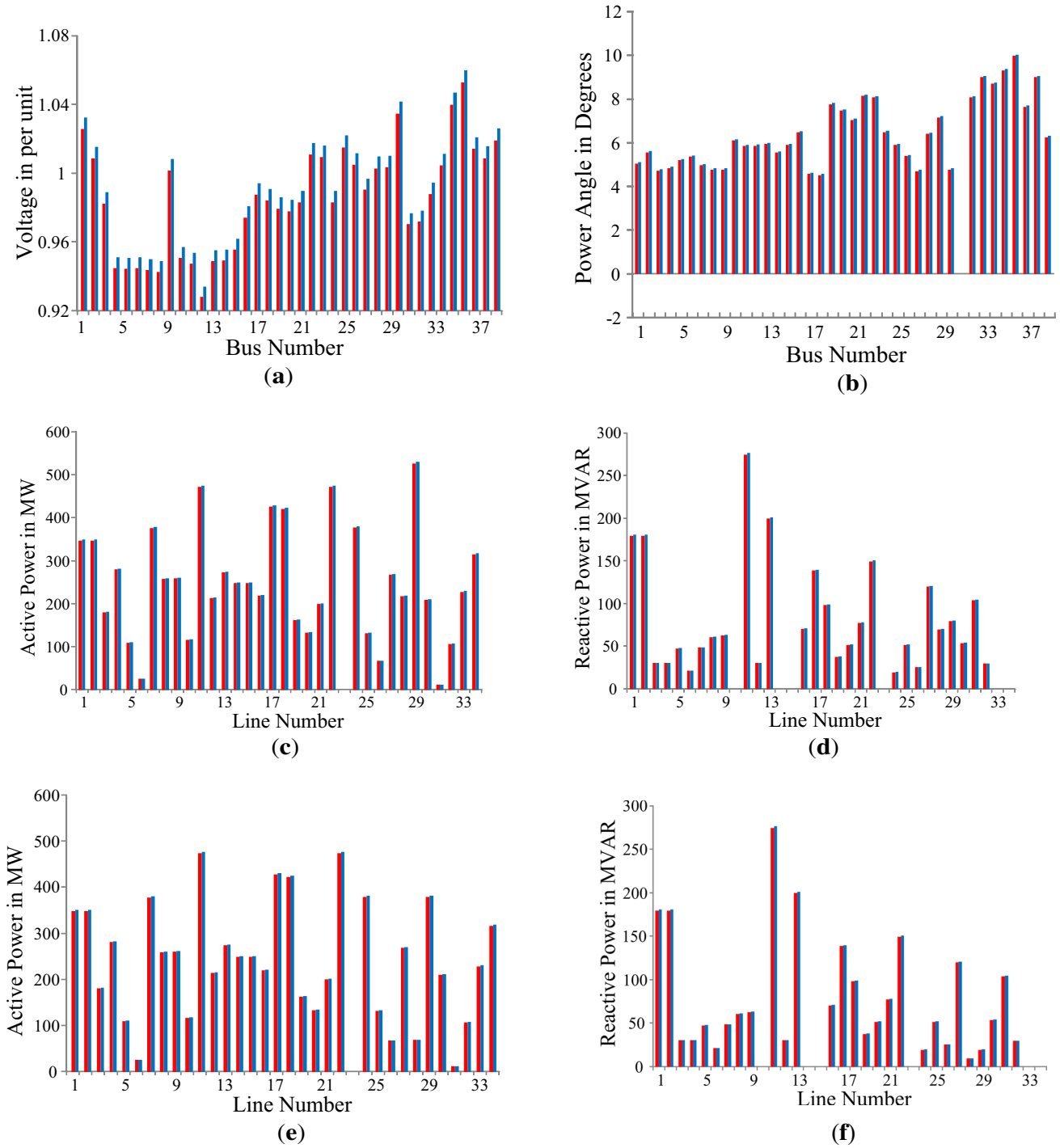

Figure 12. MATLAB and ETAP results of a test system for stable swing condition when line L-23 tripped: (**a**) bus voltage, (**b**) power angle, (**c**) active power flow, (**d**) reactive power flow, (**e**) SIPS-1 operated active power flow, and (f) SIPS-1 operated reactive power flow.

upgrade the SIPS discussed in Section 2. From (1) to (10), it is possible to segregate faults from the power swing. Therefore, the unsought trippings of transmission lines could be avoided. From the functional investigation discussed in Section 2, the SIPS operation also results in (i) heavy load curtailment and (ii) excess back-down of alternators. This is because the availability under loading conditions of transmission lines is not known. In this study,

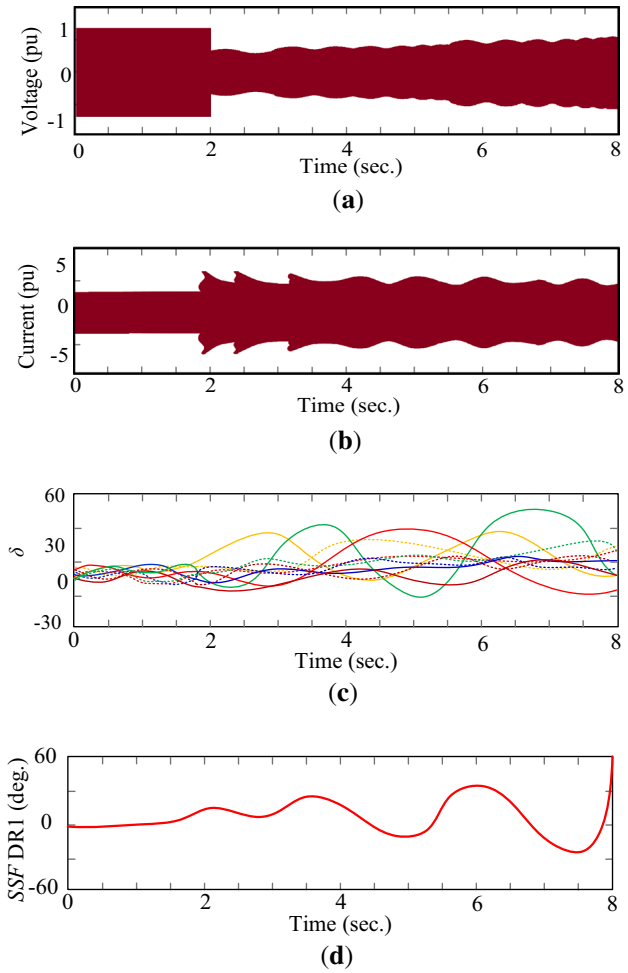

Figure 13. Functional investigation of SIPS-1 under unstable swing condition: (**a**) voltage monitored by DR1, (**b**) current seen by DR1, (**c**) variations in the angles of generating units, and (**d**) *SSF* within bus 16 and 19.

to minimize load shedding and cut generation from alternators, PMU data is used to access the under-loading of all transmission lines.

Zone-2 and zone-3 act as backup protection in distance relay. The protective elements of these zones initiate a trip command to the respective circuit breaker after 350 and 700 ms. Thus, if any fault (L-G or L-L) appears, it is always sensed by these backup elements. When the phase-a to ground fault occurs during a power swing (either in zone-2 or zone-3), there is a deviation in phase-a current. This variation (ΔI_{ij-a}) is measured by the backup relay. In case of a no-fault on phase-b and phase-c, the differences ΔI_{ij-b} and ΔI_{ij-c} will be equal and zero. These differences distinguish between the power swing and the fault and also select the faulty phase. If the primary relaying fails to operate, the backup relay initiates the trip signal to the respective circuit breaker after a predefined delay. Therefore, the proposed scheme works effectively.

Let N and M be the respective EHV AC and HVDC transmission lines. These EHV AC and HVDC lines either enter or start from the substations. The maximum power transfer capacity of these lines is expressed as

$$P_{ACmax} = \sum_{i-1}^{N} P_{AC}(i) \quad \text{(for EHV AC lines)} \tag{11}$$

$$P_{DCmax} = \sum_{j-1}^{M} P_{DC}(j) \quad \text{(for HVDC lines)} \tag{12}$$

In practice, EHV AC and HVDC lines operate such that $n \leq N$ and $m \leq M$. Thus, the actual transformations by these lines are given as

$$P_{AC} = \sum_{i-1}^{n} P_{AC}(i) \quad \text{(for EHV AC lines)} \tag{13}$$

$$P_{DC} = \sum_{j-1}^{m} P_{DC}(j) \quad \text{(for HVDC lines)} \tag{14}$$

Equations (13) and (14) determine the under-loading factors as follows:

$$UF_{AC} = \frac{P_{ACmax} - P_{AC}}{P_{ACmax}} \tag{15}$$

$$UF_{DC} = \frac{P_{DCmax} - P_{DC}}{P_{DCmax}} \tag{16}$$

These under-loading factors are used (i) to maintain the system stability, (ii) to minimize the excessive generation back-down, and (iii) thereby avoid load shedding. Subroutines 1 and 2 deal with two issues. The first is discriminations of faults and power swing. The second is the under-utilization of EHV AC and HVDC transmission lines. These two subroutines are attached to three operating SIPS discussed in Section 2. Figure 7 gives the sequence of operations with these subroutines. The testing of these suggested subroutines and their validations are in successive sections.

4. Results and discussion with relevant cases

IEEE 10-generator 39-bus arrangement with HVDC line is considered as a test system for this study depicted in figure 8. It considers bus 30 to bus 39 as PV buses, and bus 31 is the slack bus. Rest of the buses are PQ buses. This test system possesses 19 loads and 34 transmission lines. The power and voltages are in per unit (pu) with a respective base of 100 MVA and 345 kV. The π equivalent circuit line model is adopted. There are nine voltage control transformers out of twelve transformers in the test system. Each transformer has eight tap positions and the voltage is controlled from the primary side. Three SIPS described in Section 2 are assiduously tested on this test system. MTDC ingrained with this test system has two converter stations.

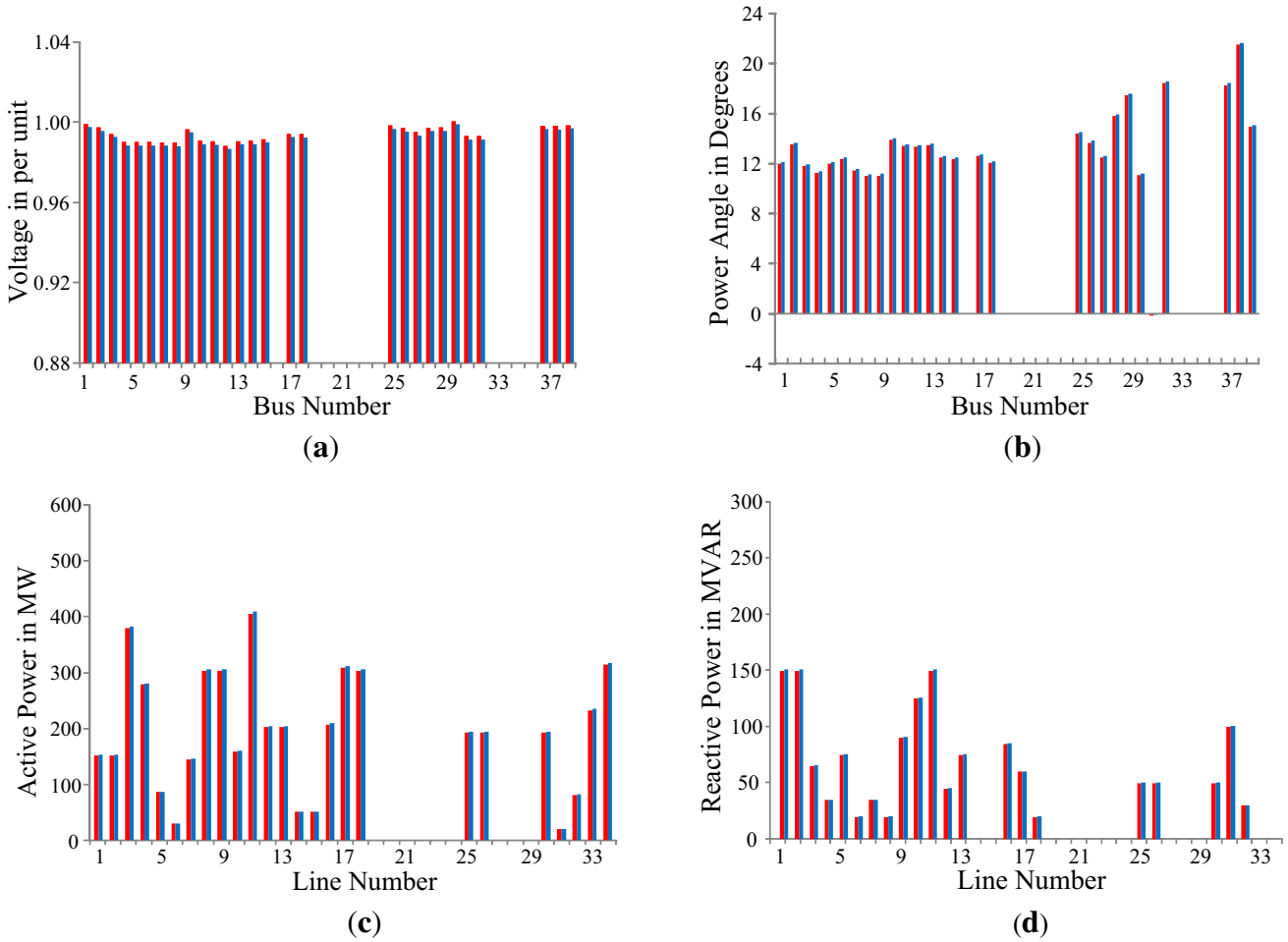

Figure 14. MATLAB and ETAP results of the test system for unstable swing condition when a fault in line L-23 not removed: (**a**) bus voltage, (**b**) power angle, (**c**) active line power, and (**d**) reactive line power.

Considering the economic constraints, PMUs are installed at bus 2, 5, 6, 9, 12, 16, 19, 22, 23, 25, 29, and 39. The test system is assembled in MATLAB®. At the earlier stage, the power flow study is carried out to verify the similarity with the practical cases. The power generation and MVA load attached to buses are in table 5. General procedures are followed for this dynamic simulation. After checking the operation of a test system, the functional behaviors of three SIPS are tested. The data received by relays DR1, DR2, and DR3 for the respective SIPS is used for the functional evaluation.

4.1 *Functional investigation of SIPS-1*

SIPS-1 is checked without and with suggested subroutines to verify its ability to restrain system instability under steady and contingency conditions. Test relay 1 (DR1) is established at E location near bus 19 on line L-22. The test system operates in MATLAB®. Bus 31 is a slack bus with a power angle equal to zero. The voltage and power angle at every bus and power flows through all lines are given in figure 9 for the normal condition. Figure 9(a) and (b) shows respective voltages and currents recorded by DR1. Figure 9(c) and (d) indicates that the system is under stable condition. All the power angles to generating units are reconciled, and hence *SSF* is found within a limit. This test system with the HVDC link was reassembled in ETAP [33] to justify the functional investigation. This test system results in ETAP are checked with MATLAB results as given in figure 10. The voltages perceived from figure 10(a) for bus 16 by, respectively, MATLAB and ETAP are 0.979 and 0.986 pu. The power angles for this bus heeded from figure 10(b) are 5.794 degrees for MATLAB and 5.849 degrees for ETAP. The active powers seen from figure 10(c) for line L-23 are 193.14 MW from MATLAB and 194.88 MW from ETAP simulations. The reactive flows from these two simulations are 36.24 and 36.52 MVAR depicted in figure 10(d). The only line that carries active power of 249.98 MW is HVDC line L-15. Thus close

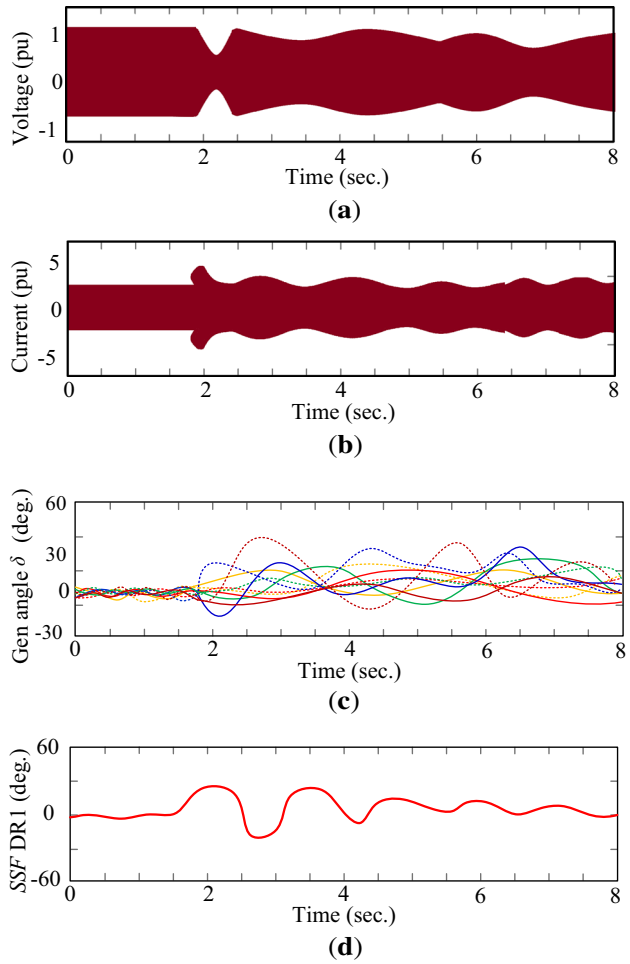

Figure 15. Functional investigation of SIPS-1 with proposed algorithm under stable power swing (**a**) voltage monitored by DR1, (**b**) current seen by DR1, (**c**) variations in the angles of generating units, and (**d**) *SSF* within bus 16 and 19.

matching of MATLAB and ETAP results is accomplished. All the transmission lines found are loaded below their rated capacity.

The symmetrical fault contrived in line L-23 between bus 16 and bus 21 causes power swing in this test system. Opening the breakers at A and B isolates this fault. The stable and unstable power swings are created by controlling this fault isolation time. The concentric circle method judges the performance. The differentiation between power swing and the fault is possible from the time elapsed to cross the impedance trajectory outer circle and zone-3 circle. The threshold time is 25 ms.

4.1.1 *Stable power swing* A triple line to ground fault (f_1) appeared at 1.8 s in line L-23 when (151+j59) MVA load was connected at bus 24 instead of defined load (312+j89) MVA. Opening breakers A and B from both ends within 85 ms isolates the fault. Thus, the constraints (5), (8), and (9) are satisfied. The power swing was present, and not fault. Test relay DR1 recorded this swing in its zone-2. Impedance trajectory took more time than the threshold to cross its zone-1 circle. Hence power swing blocking (PSB) is approved for the relays located at E, M, S, and Q.

The voltage and current waveforms under stable power swing are, respectively, in figure 11(a) and (b). The power angle of generator G6 is shifted from 8.829 to 9.314 degrees in MATLAB. This angle changes to 9.383 degrees, from 8.898 degrees in ETAP. The minute variations appearing in the angular displacement of other generation units are noticed from figure 11(c). The power swing curve mollified after 7.2 s, *SSF* is presented in figure 11(d). As line L-23 got opened, its flow became zero. The system experienced momentary disturbance. Deviation in voltages and power angles at every bus is, respectively, in figure 12(a) and (b). The power flow of L-23 shifted to its adjacent lines seen in figure 12(c) and (d). The apparent power flow of lines L-24, L-28, and L-29 boosted from (187+j17) to (383+j21), (29+j33) to (219+j71), and (339+j48) to (528+j81) MVA, respectively. However, the apparent power flow of line L-27 decreased from (460+j152) to (272+j124) MVA. Under such a scenario the system is stable, and there is no operation of SIPS. SIPS-1 activates only when the load at bus 24 exceeds 216 MVA. As soon as line L-23 underwent fault, the load at bus 16 got curtailed. This forces load cut of (312+j88) MVA and also back-down unit G6. The mutations of active power flow are in figure 12(e), and reactive power flow are in figure 12(f). The load flows of lines L-24, L-28, and L-29 heighten from (187+j17) to (381+j21), (186+j66) to (72+j12), and (494+j72) to (384+j21) MVA. However, the load flow of line L-27 decreased from (460+j157) to (271+j122) MVA. The system withstands stability by scarifying load at bus 24.

4.1.2 *Unstable power swing* The symmetrical fault (f_1) is at 2 s in line L-23. Line breaker A opened as it received a trigger signal from the associated relay. Deliberately, the opening time of another breaker B of the same line is set at 240 ms. It simulates a circuit breaker stuck situation. Hence, the tests relay DR1-sensed power swing in zone-2. Thus, the constraints (5), (8), and (9) got accosted. An unstable power swing without fault in zone-1 for relays E, M, S, and Q appeared. Therefore, the PSB feature is made active for these relays. Sticking of breaker B enables activating local breaker backup (LBB) protection for bus-bar 16. The breakers L, F, P, and R should acquire a signal from the LBB scheme and isolate bus 16. However it did not de-energies this bus as LBB protection was out of order. The impedance trajectory arrives into zone-1 of protection relays at E, M, S, and Q, and the conditions given in (5), (8), and (9) are not satisfied. The fault comes into existence due to a power swing. Relays at E, M, S, and Q got de-blocked. Tests relay DR1, and activate trip command for

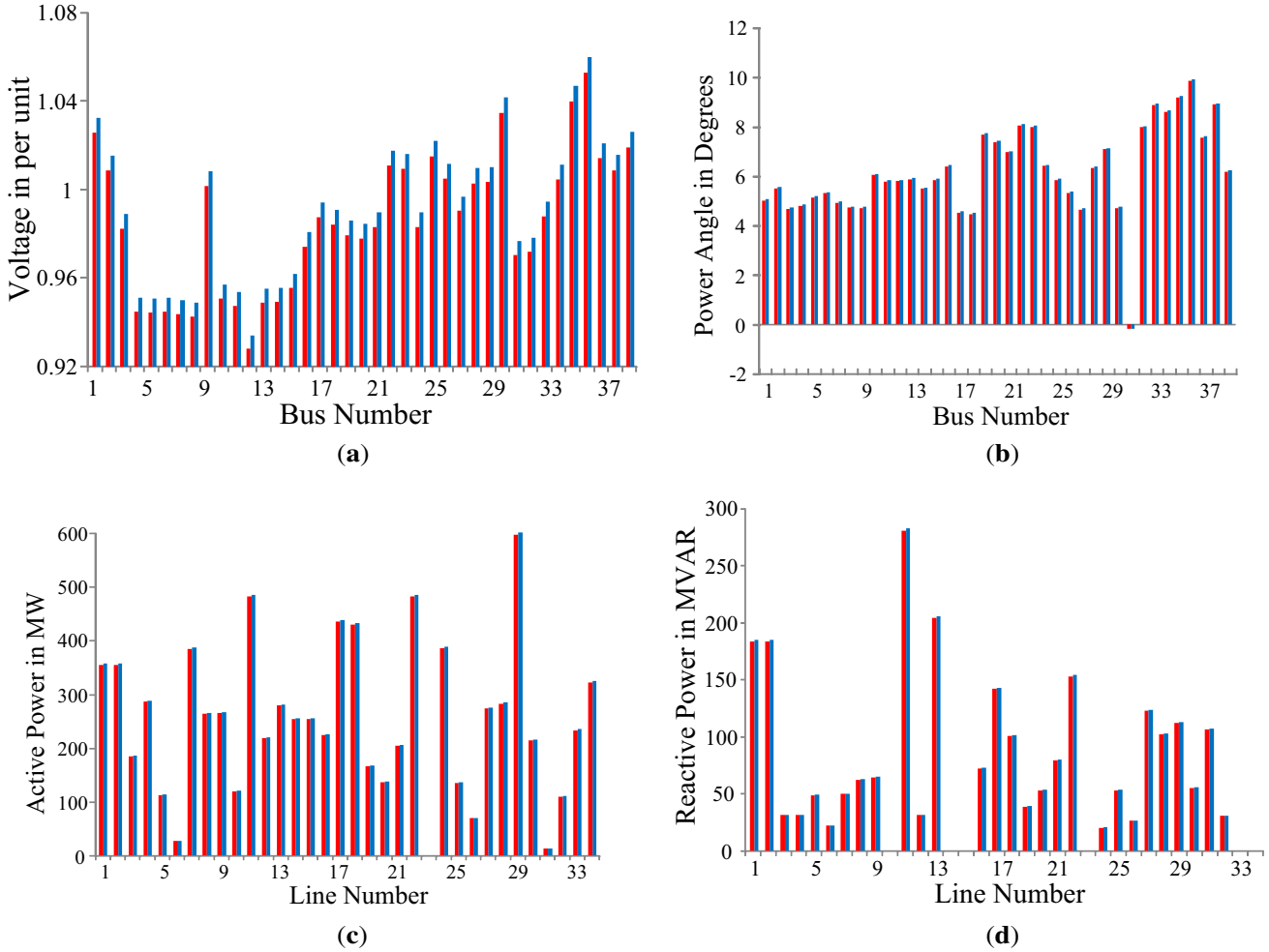

Figure 16. MATLAB and ETAP results of a test system for the stable swing when SIPS-1 executed with the proposed algorithm: (**a**) bus voltage, (**b**) power angle, (**c**) active power flow, and (**d**) reactive power flow.

breaker E. Similarly, another breaker of the remote ends fixed to bus 16 (breakers M, Q, and S) opened because of power swings and persisting fault in their zone-2. It isolates bus 16 and curtailed load of (342+j44) MVA. This isolation did not evacuate power from units G4, G5, G6, and G7. Active power loads connected at buses 20, 21, 23, and 24 did not pair with enormous generated power under such a situation. Therefore, all these alternators went out of service by OST protection.

The voltage and current waveforms, respectively, in figure 13(a) and (b) indicate an unstable power swing. The power swing (see figure 13(c)) is sensed from the angular disengagement between power angles of generators, and periodic oscillations seem to be unstable. The *SSF* has inclined towards instability found in figure 13(d). The system suffered due to instability later, 7.6 s, and it brought power to break-down in the nearby area. The dislocation of bus 16 made the blackout in that region. The change in voltage is in figure 14(a), and the angle is in figure 14(b). The relevant active power flow is in figure 14(c), and the reactive power flow for the system is shown in figure 14(d). In this SIPS logic the PSB is activated just after monitoring the swing, and it blocks all zones except zone-1. Operation of breaker A was performed correctly. However, SIPS-1 aborted as (i) breaker B of line L-23 did not open, (ii) LBB protection at bus 16 was not in service, (iii) due to a persistent fault, power swings that appeared in zone-2 did not dampen, (iv) swing that arrived in zone-1 of relays at E, M, Q, and S opened their circuit breakers, and (v) breakers W, X, Y, and Z opened due to OST activation. This investigation overcomes the discrepancy in SIPS-1 by some modifications. The modification is made clear in the coming subsection.

4.1.3 *Stable power swing with suggested subroutines* The test system operates with the earlier condition given in figure 10. All power lines are under working conditions. At 1.8 s, L-L-L fault (f_1) is aggravated

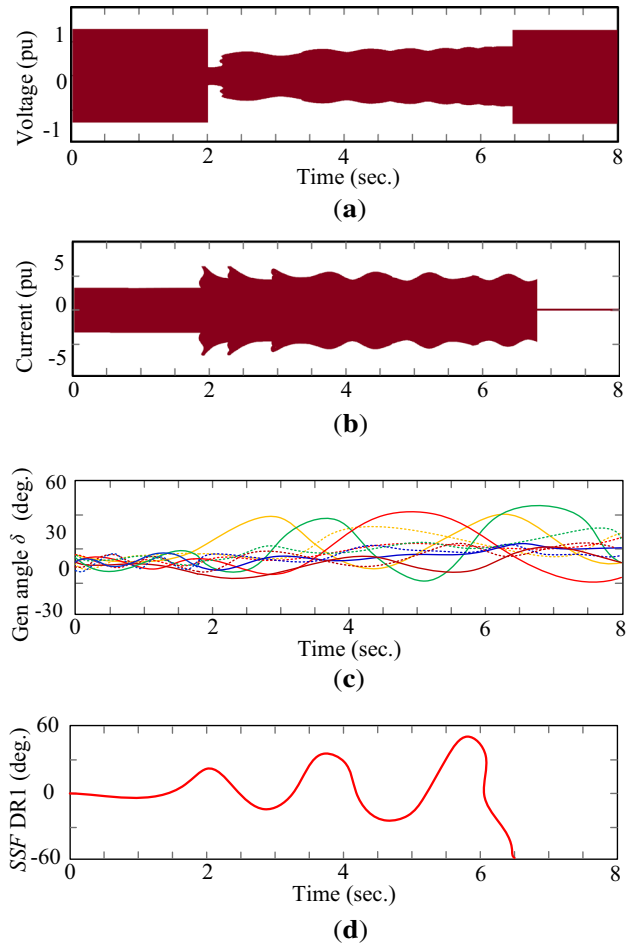

Figure 17. Functional investigation of SIPS-1 with proposed algorithm under unstable power swing: (**a**) voltage monitored by DR1, (**b**) current seen by DR1, (**c**) variations in the angles of generating units, and (**d**) *SSF* within bus 16 and 19.

in line L-23 when supplying a load of (190+j32) MVA. After 90 ms, the fault got cleared. Test relay DR1 experiences power swing in zone-2, and there is no fault in its zone-1. It effectuated (5), (8), and (9). Hence, the PSB got activated for relays at E, M, S, and Q. It forced load curtailment of 312 MW and 91 MVAR at bus 24. The power flow of line L-23 was transferred on lines L-24, L-28, and L-29. The test system remains stable because of the load cut. Transmission links L-24, L-28, and L-29 operated, respectively, at 63.5%, 11.84%, and 36.5% of their maximum power transfer capacity. Hence there is a clear possibility to transfer more power, and it reduces the load shedding.

The suggested subroutines work out and curtail load equal to 99 MW only. It prevented the load shedding of loads attached to bus 24. Now, it fed (209+j90) MVA demand at this bus. The power by L-29 heightened at 598 MVA. The corresponding voltage and current signals indicate stable swing seen, respectively, from figure 15(a) and (b). The angular displacements of other alternators shown in figure 15(c) are little. At 7.4 s, just after the load cut, the swing got mitigated. The *SSF* is in figure 15(d). After the opening of L-23, fluctuations appear in voltage and angle at other buses seen from corresponding figure 16(a) and (b). Load flows are in figure 16(c) and (d). This sustained stability is because of the correct execution of SIPS-1 with limited load shedding.

4.1.4 *Unstable power swing with suggested subroutines* The investigation of PMU technology made it easy to access the rotor angle of generating unit. This information supports grid management. Due to a weird exigency, the prominence of the generation load angle and its variation are higher than in a regular emergency. In the test system, an unstable swing is ascertained by DR1 when the L-L-L fault continues for a long duration of 500 ms in line L-23. It pushed the system towards instability. However, the curative measures commenced at an exact instant and to prevent system instability. While accrediting these modifications, it has to be confirmed that protection operates for every fault in power swing.

In the power swing state, a three-phase fault (f_1) is in line L-23 at 1.9 s. After 85 ms, by opening relevant circuit breakers, this fault is removed. Breaker A opened, but breaker B got stuck. Relay DR1 fixed at E and other relays at M, Q, and S revealed this fault in zone-2 with power swing. The recommended flowchart is with SIPS-1. LBB protection of bus 16 is not operative. After checking *SSF*, the relays at E, M, Q, and S are de-blocked. These relays activate the opening of corresponding breakers and thereby isolate bus 16 from the system. The logic applied is that whenever line L-22 is open, or bus 16 is not in service, the unit G4 must get detached from the system. Under contingency, unit G4 mandatorily detached from service. Some units, G5, G6, and G7, operated by backing down their generations. It is in contrast with load at buses 20, 21, 23, and 24. It forbids unwanted outages of G5, G6, and G7. By this corrective measure, power swing is mitigated and also blackout in this area is avoided. The system achieves stable status depicted in figure 17(a), (b), (c), and (d), respectively, for the voltage, current, power angle, and *SSF*.

The angular movement observed is more than 28.2 degrees. Figure 18(a), (b), (c), and (d) illustrates parameters after isolating bus 16. The under-loading factors for L-17, L-18, and L-19 were determined, respectively, as 48.18%, 49.88%, and 99.9% by the proposed subroutine. Therefore, it partially withdraws the load shedding at bus 14. In such a situation, bus 27 is made free from the load. Bus 15 supplied (139.85+j64.15) MVA load because of the correct operation of subroutines included in SIPS. This functional response gives the following propositions: (i) revise and coordinate settings of all the protection relays, (ii) confirm operation of bus bar protection and LBB protection at each bus, (iii) perform load flow study and figure out loading factor of all lines, (iv) adjust OST protection so that it can

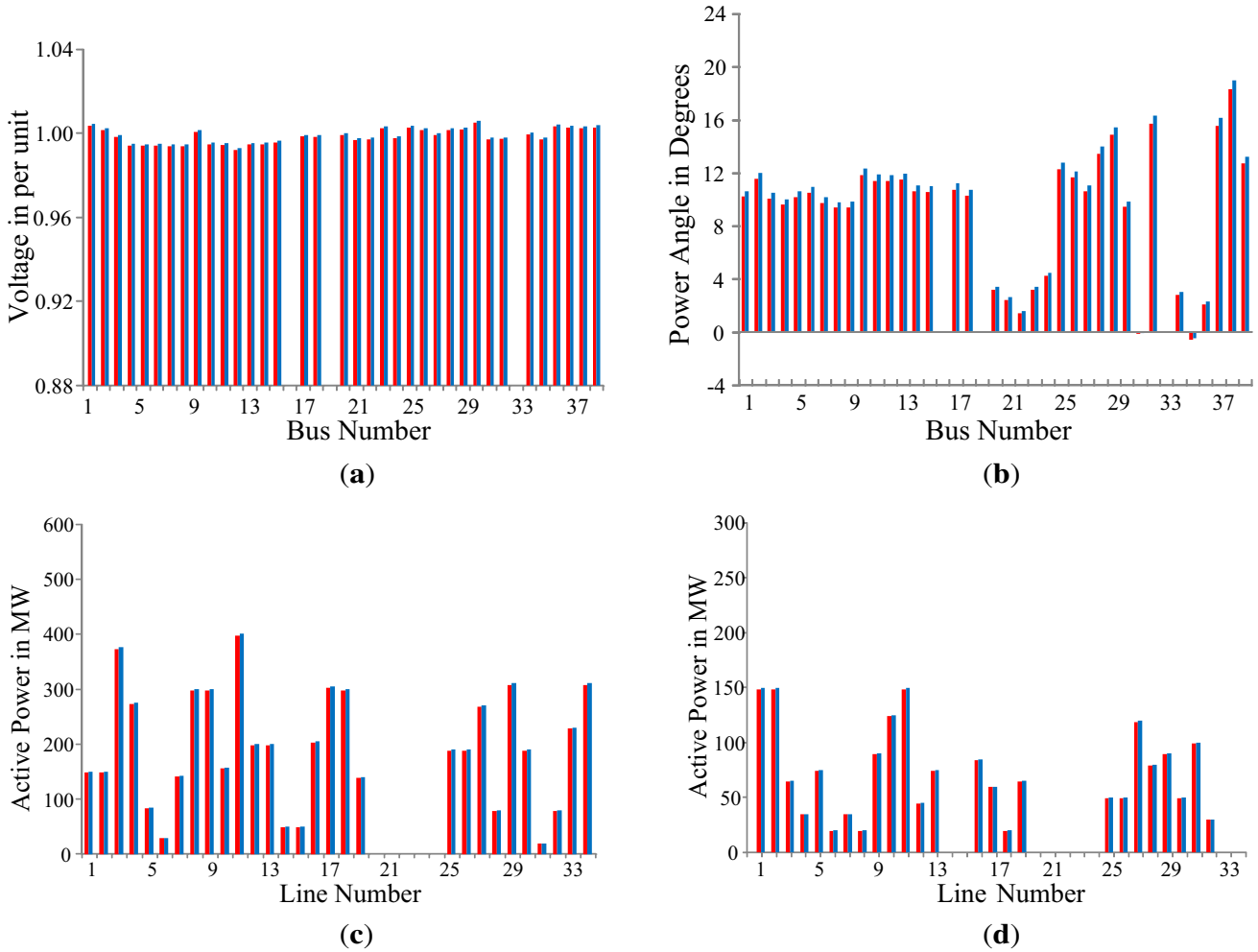

Figure 18. MATLAB and ETAP results of a test system for the unstable swing when SIPS-1 executed with a proposed algorithm: (**a**) bus voltage, (**b**) power angle, (**c**) active power flow, and (**d**) reactive power flow.

avoid unwanted trippings of generating units, and (v) backing down of generation should correlate with frequency load dropping characteristics for every generation unit.

4.2 *Functional investigation of SIPS-2*

The line to ground fault (f_2) triggered at 2.2 s in the DC line L-15 transmitting 582 MW, and the load at bus 39 was (772+j182) MVA. Both ends circuit breakers opened within 80 ms and isolated the faulty section. This fault generated momentarily power swing diagnosed by test relay DR2. The load flows of lines L-4 and L-12 due to fault are more than the threshold, i.e. 600 MVA. The maximum power transmission is restrained at 600 MVA for 400 kV because of its thermal limits. SIPS-1 operates and disconnects the load at bus 7. It also reduced the generation of unit G2 by (200 +j80) MVA. The voltage and current are, respectively, in figure 19(a) and (b). Figure 19(c) and (d), respectively, depicts the angular change and *SSF*.

The proposed subroutines determine the % under-loading factor of adjacent lines. Line L-12 is found to be 27.57% under-loaded. Subroutine 2 improved the generation backdown of G2 by (96+j36) MVA and thus decreased load shedding at bus 8 to (98+j38) MVA. MATLAB and ETAP simulation results for a few buses and lines without and with the application of the advanced subroutine are in figure 20. It is confirmed from figure 20(a) and (b) that minimizing generation back-out elevates bus voltages and diminishes angular disturbance. The improvements in active power flow and reactive power flow are, respectively, in figure 20(c) and (d).

4.3 *Functional investigation of SIPS-3*

Symmetrical (LLLG) fault (f_3) is activated at 2.2 s in line L-25 when transmitting 530 MW. Just after this fault, line L-6 started export instead of import of power to bus 3. By opening both end breakers within 90 ms, this fault is isolated. Test relay DR3 monitored a power swing for a

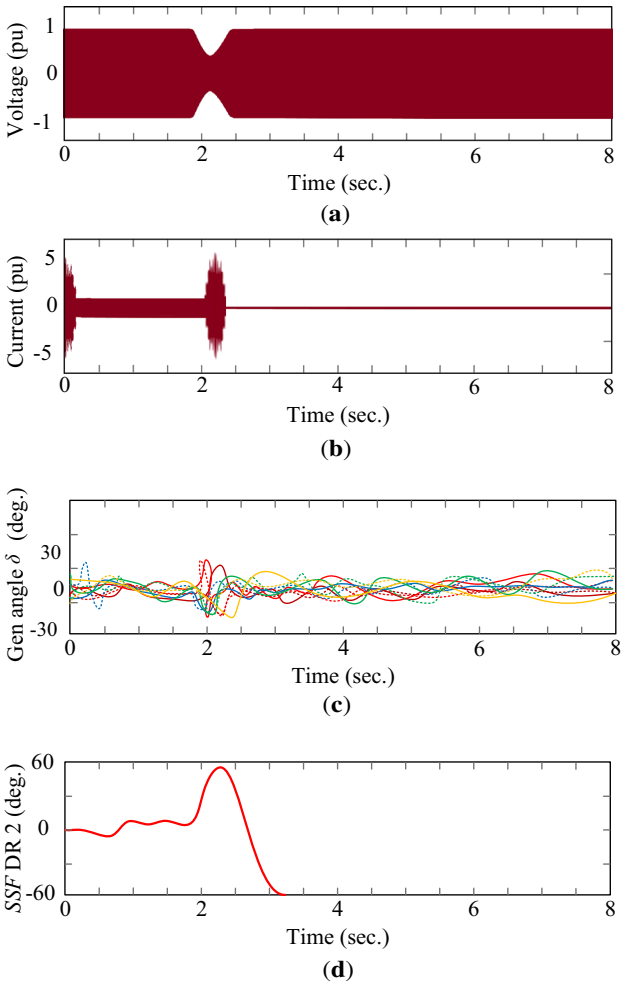

Figure 19. Functional investigation of SIPS-2: (**a**) voltage monitored by DR2, (**b**) current seen by DR2, (**c**) variations in the angles of generating units, and (**d**) *SSF* within bus 9 and 39.

moment just after this symmetrical fault. This event raises the flow through lines L-3 and L-4 to greater than 600 MW. It enabled the SIPS operation. Thus it enforced backing down of generation G8 by 352 MW. It cuts the entire load at bus 18 and reduces the load at bus 3 to 122 MW. The voltage and current for this performance are, respectively, in figure 21(a) and (b); the angular movements and *SSF* are seen in figure 21(c) and (d). The proposed subroutine computed that lines L-3 and L-4 are 21.53 % and 30.1 %, respectively, less loaded. Therefore, another subroutine 2 is executed. It forces a reduction in the generation of G1 by 101 MW. The load at bus 3 is shed to 42 MW. It managed an 80 MW load at bus 18 against complete load shedding. The MATLAB and ETAP results for some buses and lines without and with suggested subroutines are in figure 22.

In this study, the authors have simulated similar conditions that appear in practical cases. By simulation study, three power system events have been analyzed. Performance of these events is checked on IEEE 10 generators 39-bus test system ingrained with HVDC link. Further, the proposed methodology constituted with two subroutines is proposed to overcome the drawbacks of currently working SIPS. The performance of this algorithm is tested in MATLAB and validated in ETAP. Simulation results in both environments match closely.

The summary of this investigation is as follows:

1. Functional investigation of three SIPSs made on IEEE 10 generators 39-bus test system ingrained with HVDC link.
2. Proposed subroutines use PMU data to improve the decision-making about blocking and de-blocking function in distance relays. It boosts the performance of these SIPSs.
3. The recommended scheme did not require any prediction system or estimation model. However, it works effectively under critical situations.
4. Proposed subroutines prevent unwanted load shedding and forced outages of generating units to a maximum extent.
5. Performance results explore the causes behind right and wrong SIPS operations. MATLAB results are compared to ETAP results for validation.

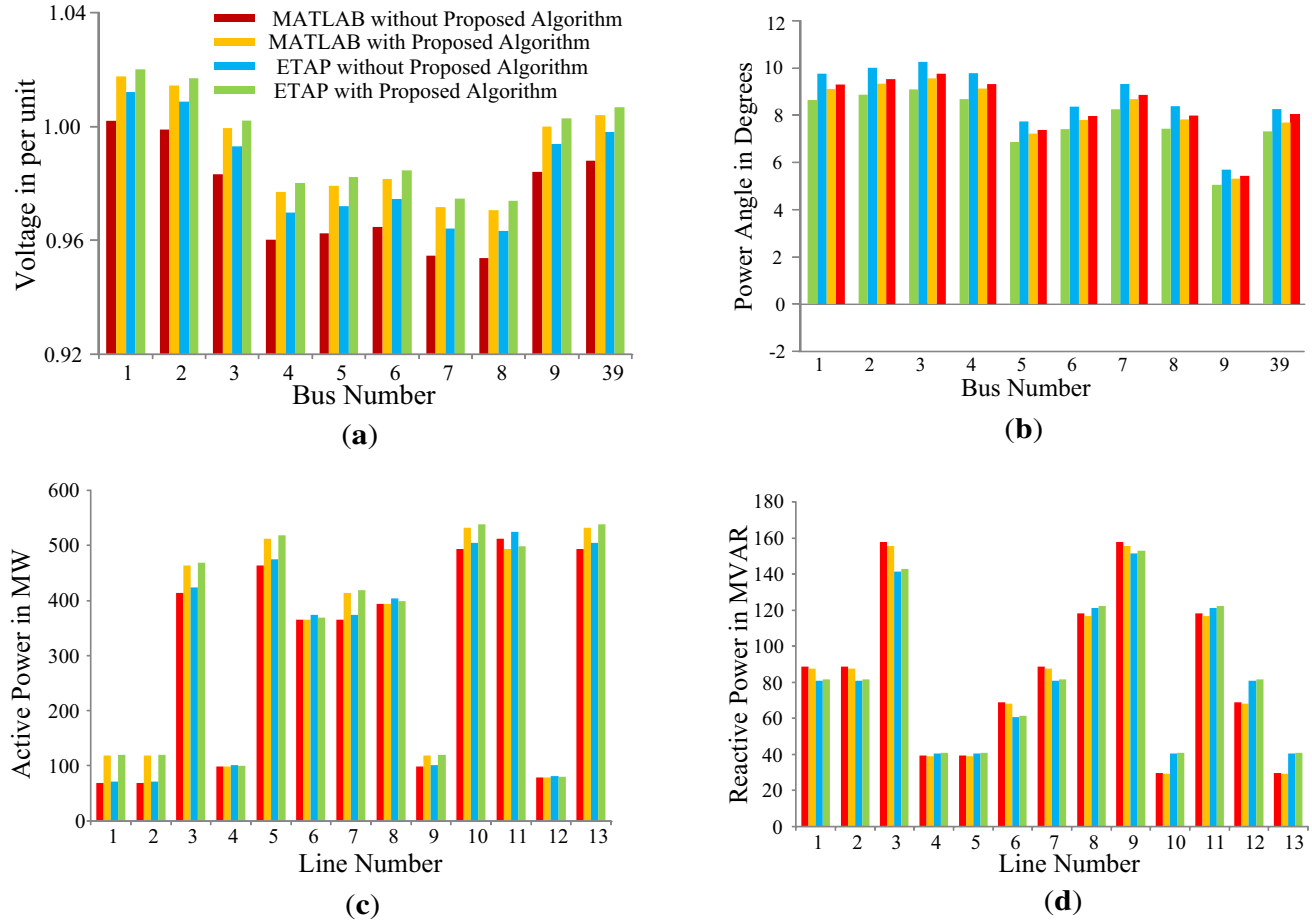

Figure 20. MATLAB and ETAP results of SIPS-2 without and with the application of proposed algorithm: (**a**) bus voltage, (**b**) power angle, (**c**) active power flow, and (**d**) reactive power flow.

5. Conclusion

Three SIPSs in the Indian power grid were simulated and analyzed in this article. It investigates the demerits in these three currently operating SIPSs. Two proposed subroutines resolved these discrepancies. PMU data was required for these two subroutines. They avert the complex estimation modeling and thereby the possibility of probable errors. One subroutine separates the power swing from the fault and prevents abnormal trippings of transmission lines. Another subroutine estimates the under-loading factor of every EHV AC and HVDC line and thereby abstains from the disproportionate load shedding and back out of generating units. These three SIPS are meticulously tested by developing the IEEE 10 generators 39-bus test system ingrained with HVDC link in MATLAB and ETAP without

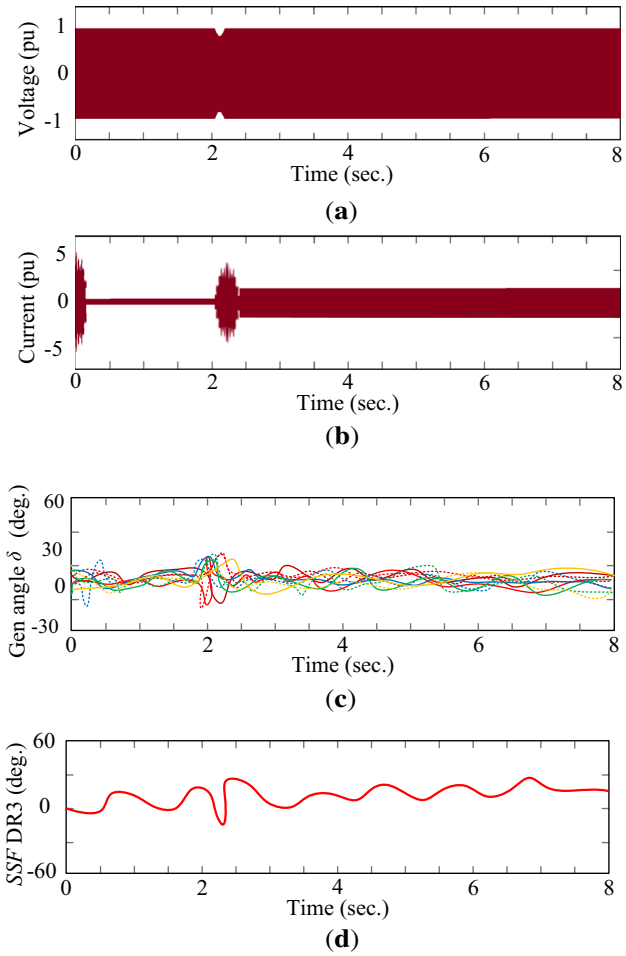

Figure 21. Functional investigation of SIPS-3: (**a**) voltage monitored by DR3, (**b**) current seen by DR3, (**c**) variations in the angles of generating units, and (**d**) *SSF* within bus 2 and 25.

and with proposed subroutines. Their results prove the technical feasibility of the proposed methodology.

Acknowledgements

Maharashtra State Electricity Transmission Company Limited (MSETCL), Mumbai.

Listy of symbols

Abbreviations

SIPS	System integrity protection schemes
CGPL	Coastal Gujarat Power Limited
UMPP	Ultra-mega-power plant
OLD	One-line diagram
ER	Eastern region
WR	Western region
NR	Northern region
KTPS	Korba Thermal Power Station
PMU	Phasor measurement unit
SSF	System stability factor
MTDC	Multi-terminal DC
DR	Distance relay
ETAP	Electrical Transient Analyzer Program
L-G	Line to ground fault
L-L-L	Three-phase line fault
OST	Out of step

Parameters and variables

$v(t)$	Voltage signal
V_i	RMS values of i^{th} bus voltage
V_j	RMS values of j^{th} bus voltage
θ_i	Phase angle at i^{th} bus
θ_j	Phase angle at j^{th} bus

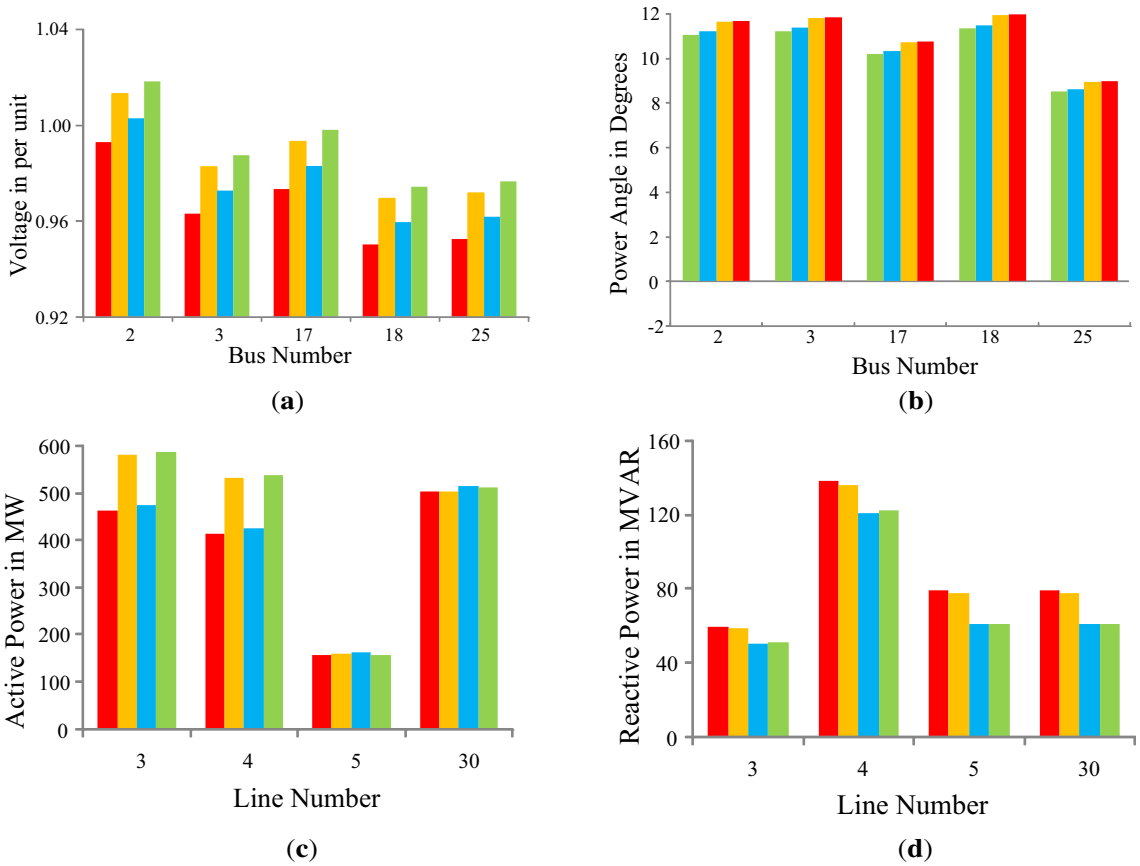

Figure 22. MATLAB and ETAP results of SIPS-3 without and with the application of proposed algorithm: (**a**) bus voltage, (**b**) power angle, (**c**) active power flow, and (d) reactive power flow.

ΔV_{ij}	Differential voltage
ΔI_{ij}	Differential current
ΔZ_{ij}	Change of impedance
δ_{ij}	Angular separation between bus i and bus j
$\delta_{ij(max)}$	Maximum angular separation
T	Define time interval
ΔZ_1	Change in impedance seen by the relay in zone-1
ΔZ_2	Change in impedance seen by the relay in zone-2
ΔZ_3	Change in impedance seen by the relay in zone-3
N	Maximum EHV AC transmission lines in a substation
M	Maximum HVDC transmission lines in a substation
n	EHV AC transmission lines in service
m	HVDC transmission lines in service
P_{ACmax}	Maximum power transmission capacity of EHV AC lines
P_{DCmax}	Maximum power transmission capacity of HVDC lines
P_{AC}	Actual power transmission capacity of EHV AC lines
P_{DC}	Actual power transmission capacity of HVDC lines
UF_{AC}	Under-loading factor of EHV AC lines in the percentage
UF_{DC}	Under-loading factor of HVDC lines in the percentage

References

[1] Goossens M, Mittelbach F and Samarin A 1993 *The LaTeX companion*. Reading, Massachusetts: Addison-Wesley

[2] Zobaa A F and Vaccaro A (Eds.) 2014 Computational intelligence applications in smart grids: enabling methodologies for proactive and self-organizing power systems. *World Scientific*

[3] Häger U, Rehtanz C and Voropai N 2014 *Monitoring, control and protection of interconnected power systems*. New York: Springer

[4] Horowitz Stanley H and Phadke Arun G 2008 *Power system relaying*. England: *Wiley*,

[5] Das J C 2010 *Transients in electrical systems: analysis, recognition, and mitigation*. McGraw Hill Professional

[6] Begovic Miroslav M 20212 *Electrical transmission systems and smart grids: selected entries from the Encyclopaedia of Sustainability Science and technology*. New York: Springer

[7] Anderson P M and LeReverend B K 1996 Industry experience with special protection schemes. *IEEE Trans. Power Syst.* 11(3): 1166–1179, https://doi.org/10.1109/59.535588

[8] Taylor CW, Erickson D C, Martin K E, Wilson R E and Venkatasubramanian V 2005 WACS—wide-area stability and voltage control system: R&D and online demonstration. *Proc. IEEE* 93: 892–906, https://doi.org/10.1109/JPROC.2005.846338

[9] Chunju F, Xiuhua D, Shengfang L and Weiyong Y 2007 An adaptive fault location technique based on PMU for transmission line. In: *Proceeding of the IEEE Power Engineering Society General Meeting*, Tampa, Florida, USA, https://doi.org/10.1109/PES.2007.385545

[10] Chompoobutrgool Y, Vanfretti L and Ghandhari M 2011 Survey on power system stabilizers control and their prospective applications for power system damping using Synchrophasor-based wide-area systems. *Eur. Trans. Electr. Power* 21(8): 2098–2111

[11] Gao W and Ning J 2011 Wavelet-based disturbance analysis for power system wide-area monitoring. *IEEE Trans. Smart Grid* 2(1): 121–130. https://doi.org/10.1109/TSG.2011.2106521

[12] Korkali M, Lev-Ari H and Abur A 2012 Traveling-wave-based fault location technique for transmission grids via wide-area synchronized voltage measurements. *IEEE Trans. Power Syst.* 27(2): 1003–1011. https://doi.org/10.1109/TPWRS.2011.2176351

[13] Hillberg E, Trengereid F, Breidablik A, Uhlen K, KjØlle G *et al* System integrity protection schemes – increasing operational security and system capacity. In: *Proceedings of CIGRE 2012*, http://www.cigre.org

[14] Panteli M, Crossley P A and Fitch J 2015 Design of dependable and secure system integrity protection schemes. *Int. J. Electr. Power Energy Syst* 68: 15–25. https://doi.org/10.1016/j.ijepes.2014.12.047

[15] Feng G and Abur A 2016 Fault location using wide-area measurements and sparse estimation. *IEEE Trans. Power Syst.* 31(4): 2938–2945. https://doi.org/10.1109/TPWRS.2015.2469606

[16] Kundu P and Pradhan A K 2016 Enhanced protection security using the system integrity protection schemes (SIPS). *IEEE Trans. Power Delivery* 31(1): 228–235. https://doi.org/10.1109/TPWRD.2015.2459231

[17] Leger A S *et al* 2016 Smart grid test-bed for Wide-Area Monitoring and Control systems. In: *Proceedings of the 2016 IEEE/PES Transmission and Distribution Conference and Exposition (T&D)*, IEEE

[18] He J *et al* 2016 Development and research on integrated protection system based on redundant information analysis. *Prot. Control Mod. Power Syst.* 1: 13, https://doi.org/10.1186/s41601-016-0024-y

[19] Kim D I, Chun T Y, Yoon S H, Lee G and Shin Y J 2017 Wavelet-based event detection method using PMU data. *IEEE Trans. Smart Grid* 8(2): 1154–1162. https://doi.org/10.1109/TSG.2015.2478421.

[20] Liu N and Crossley P A 2018 Assessing the risk of implementing system integrity protection schemes in a power system with significant wind integration. *IEEE Trans. Power Deliv.* 33(2): 810–820. https://doi.org/10.1109/TPWRD.2017.2759181

[21] Hashemi S M, Sanaye-Pasand M and Shahidehpour M 2018 Fault detection during power swings using the properties of fundamental frequency phasors. *IEEE Trans. Smart Grid* 10(2): 1385–1394. https://doi.org/10.1109/TSG.2017.2765200

[22] Kumar D S and Savier J S 2019 Synchrophasor based system integrity protection scheme for an ultra-mega power project in India. *IET Gener. Transm. Distrib.* 13(8): 1220–1228. https://doi.org/10.1049/iet-gtd.2018.5510

[23] Gawande P and Dambhare S 2019 New predictive analytic-aided response-based system integrity protection scheme. *IET Gener. Transm. Distrib.* 13(8): 1204–1211, https://doi.org/10.1049/iet-gtd.2018.5585

[24] Unde S, Gawande P and Dambhare S. New algorithm for protection of double circuit transmission lines using modal currents. *IEEE Trans. Power Delivery* 34(5): 1967–1977, https://doi.org/10.1109/TPWRD.2019.2906939

[25] Ravikumar K G and Srivastava A K 2019 Designing centralised and distributed system integrity protection schemes for enhanced electric grid resiliency. *IET Gener. Trans. Distrib.* 13(8): 1194–1203. https://doi.org/10.1049/iet-gtd.2018.5381

[26] Sahoo B and Samantaray S R 2020 System integrity protection scheme for enhancing backup protection of transmission lines. *IEEE Syst. J.*

[27] Skok S and Ivankovic I 2019 System integrity protection schems for future power transmission system using synchrophasors. In:*Proceedings of Smart Grid Synchronized Measurements and Analytics (SGSMA)*, https://doi.org/10.1109/SGSMA.2019.8784463

[28] Zbunjak Z and Kuzle I 2019 System integrity protection scheme (SIPS) development and an optimal bus-splitting scheme supported by phasor measurement units (PMUs). *Energies* 12(17): 3404, https://doi.org/10.3390/en12173404

[29] Mehrabankhomartash M, Saeedifard M and Grijalva S 2020 Model predictive control based AC line overload alleviation by using multi-terminal DC grids. *IEEE Trans. Power Syst.* 35(1): 177–187, https://doi.org/10.1109/TPWRS.2019.2927548

[30] Mallikarjuna B and Maddikara J B R 2020 Synchrophasor measurement assisted system integrity protection scheme for smart power grid. *J. Control Automat. Electr. Syst.* 31: 207–225, https://doi.org/10.1007/s40313-019-00516-4

[31] Wang P and Govindarasu M 2020 Multi agent based attack resilient system integrity protection for smart grid. *IEEE Trans. Smart Grid* (Early Access) https://doi.org/10.1109/TSG.2020.2970755

[32] Central Electricity Regulatory Commission [online]. Available: https://www.cercind.gov.in/

[33] Western Regional Power Committee [online]. Available: https://www.wrpc.gov.in/

[34] E-Tap 7.0.0 Demo Guide by Operation Inc. [online]. Available: http://docshare04.docshare.tips/files/